Control of Human Induced Floor Vibrations

by

Sean Manuel Homem

Bachelor of Science in Civil Engineering
Merrimack College, 2006

Submitted to the Department of Civil and Environmental Engineering
in Partial Fulfillment of the Requirements for the Degree of

MASTER OF ENGINEERING
in Civil and Environmental Engineering

at the

MASSACHUSETTS INSTITUTE OF TECHNOLOGY

June, 2007

Signature of Author: _____
Department of Civil and Environmental Engineering
May 21, 2007

Certified by: _____
Professor Jerome J. Connor
Department of Civil and Environmental Engineering
Thesis Supervisor

Accepted by: _____
Professor Daniele Veneziano
Chairman, Departmental Committee for Graduate Students

Control of Human Induced Floor Vibrations

by

Sean Manuel Homem

Submitted to the Department of Civil and Environmental Engineering on May 21, 2007 in partial fulfillment of the requirements for the Degree of Master of Engineering in Civil and Environmental Engineering.

ABSTRACT

With the growing demand for open, column-free floor spaces and the advances in material strength, floor vibration serviceability criterion has been of growing importance within the past 20-30 years. All floor systems are flexible and when introduced to a dynamic loading respond in a vibratory manner. The issues with floor serviceability arise when the floor vibrates in an uncomfortable way when exposed to everyday loading, for example human footfall in an office building. Vibrating floors have been divided into 4 categories based on the perceptibility by humans: (a) vibration, though present, is not perceived by the occupants; (b) vibration is perceived but it does not annoy the occupant; (c) vibration annoys and disturbs; (d) vibration is so severe that it makes people sick. This thesis is focused on the control of human induced floor vibrations. In order to provide the reader with practical insight on the subject, a case study of an existing steel framed office building that experienced excessive and annoying floor vibrations will be discussed and analyzed. As a result of this case study, it has been determined that the Alan and Rainer scale, along with the Modified Reiher Meister scale and the Wiss and Paremelee scale, accurately describe the human response criteria. Also determined was that the American Institute of Steel Construction Floor Vibrations Due to Human Activity (Design Guide 11) has extremely conservative acceleration criteria that basically aim to make the vibration not noticeable at all.

Thesis Supervisor: Jerome J. Connor

Title: Professor, Department of Civil and Environmental Engineering

Acknowledgements

I would like to take this opportunity to thank the Department of Civil and Environmental Engineering staff for making my experience here unforgettable.

To the MEng. Class of 2007, you are a wonderful group of intelligent and sincere people. I am extremely sad that we will part ways, but I am honored to have shared these memories with you and look forward to our continued network of personal and professional relationships.

Special thanks to the core crew that always had time for a little fun once the work was done. Alejandro, Bahjat, Andres, and Ioannis we had an amazing time this year, seriously.

Thanks to the steel bridge crew, I learned so much from you all and I feel privileged to have worked with you this year.

Gavin, Steve, Luca, and the rest of the crews, you are the best and thanks for bearing with my absence this year.

I want to thank Professor Connor for his support and kindness. You are truly a brilliant and insightful person to whom I am extremely grateful.

To Professor Anthony Deluzio, I could not have done this without you. I am extremely grateful for all that you have taught both in and out of the classroom. Thank you for your continued support, generosity, and shared wealth of knowledge.

Sabrina, thank you for your support and patience throughout this entire year. You are absolutely breathtaking and I am blessed to have you in my life. I love you.

To my family I dedicate this thesis to you. To my father, Manuel, mother, Bonnie, and sister, Ashley, I am the luckiest person in the world to have such an amazing family. I love you all.

1. Introduction and Scope 4
2. The Nature of Human Induced Vibration 6
2.1. Basic Principles of Structural Dynamics 6
2.2. Properties of Continuous Beams 11
2.3. Dynamic Loading 13
2.4. Response to Periodic Excitation 14
2.5. Human Induced Loading and the Consequent Response 20
3. Design Aids and Suggestions 24
3.1. Human Response Criteria 25
3.1.1. Modified Reiher and Meister Scale 25
3.1.2. Wiss and Parmelee 27
3.1.3. Canadian Standards Association Scale 28
3.1.4. Murray Criterion 29
3.1.5. International Organization for Standardization Scale 30
3.2. Vibration Design Criteria for Steel Beam-Concrete Slab Construction 30
4. Floor Vibration Case Study: Bank in Massachusetts 32
4.1. Background Information and Introduction to Vibration Problem 32
4.2. Data Collection (1988 Testing), Analysis, and Consequent Retrofit 33
4.2.1. Data Collection and Analysis 33
4.2.2. Consequent Retrofit 40
4.3. Current Status of Floor System 43
4.4. Past Data Present Data 54
4.5. Alternative Design to Control Floor Vibration 55
4.6. Conclusions and Recommendations 66
5. Conclusions 67
6. References 68
7. Appendix A: List of Acceptance Criteria (Murray et al.) 69
8. Appendix B: Structural Calculations 70
9. Appendix C: Development of Tuned Mass Damper Design Charts 75
10. Appendix D: Tuned Mass Damper Design Calculations 86

Figure 2-1: Single Degree of Freedom System (Connor, 9) 6
Figure 2-2: Typical a.) Beam and b.) Floor System Mode Shapes (Murray et al., 3) 8
Figure 2-3: Free Vibration of a System without Damping (Chopra, p. 40) 9
Figure 2-4: Effects of Damping on Free Vibration (Chopra, p. 50) 9
Figure 2-5: Free Vibration Response with Different Levels of Damping (Chopra, 51) 10
Figure 2-6: Free Vibration of Underdamped, Critically Damped, and Overdamped Systems (Chopra, 49) 11
Figure 2-7: Natural Vibration Modes and Frequencies of Uniform Simply Supported Beams (Chopra, 635) 12
Figure 2-8: Types of Dynamic Loading (Murray et al., 2) 13
Figure 2-9: Plot of H_1 versus Frequency Ratio, ρ, and Damping Ratio, ξ (Connor, 11) 16
Figure 2-10: Plot of H_2 versus Frequency Ratio, ρ, and Damping Ratio, ξ (Connor, 13) 17
Figure 2-11: Acceleration Controlled Design Example 19
Figure 2-12: Force-Time Curves for Walking Body, Vertical Forces (Smith, 287) 21
Figure 2-13: Force-Time Curves for Walking Body, Combined Vertical Forces (Smith, 287) .. 21
Figure 2-14: Sample Time History Plot and Frequency Spectrum (Hanagan et al., 128) 23
Figure 3-1: Modified Reiher-Meister Scale (Murray, 63) 26
Figure 3-2: Comparison of Modified Reiher-Meister and Wiss-Parmelee scales (Murray, 83) ... 28
Figure 3-3: Canadian Standards Association Scale developed by Allen and Rainer (Murray et. al, 69) 29
Figure 3-4: ISO Scale (Murray et al., 69) 30
Figure 4-1: Acceleration Time-History and Frequency Spectrum (John walking) 35
Figure 4-2: Acceleration Time-History and Frequency Spectrum (Tony walking) 36
Figure 4-3: Acceleration Time-History and Frequency Spectrum (Sheila walking) 37
Figure 4-4: Acceleration Time-History and Frequency Spectrum (30 lb. dropped 2 ft.) 38
Figure 4-5: Steel Joist and Metal Deck (Homem) 39
Figure 4-6: Schematic Drawing of Preloaded Slender Rod and Concrete Slot Detail 42
Figure 4-7: Rod Connection with Bottom Flange of Steel Joist (Homem) 42
Figure 4-8: Series of Preloaded Rods (Homem) 43
Figure 4-9: Floor with Vibration Issue and Partitions Added (Homem) 44
Figure 4-10: a.) Low-g Accelerometer b.) LabPro Transfer Device 45
Figure 4-11: Acceleration Time-History (above) and Frequency Spectrum (below) (Colin Walking Heavily) 46
Figure 4-12: Acceleration Time-History (above) and Frequency Spectrum (below) (Tony Walking) 47
Figure 4-13: Acceleration Time-History (above) and Frequency Spectrum (below) (Tony Jumping) 48
Figure 4-14: System Response with Acceptable Acceleration Criteria (Colin Walking) 52
Figure 4-15: System Response with Acceptable Acceleration Criteria (Tony Walking) 52
Figure 4-16: System Response with Acceptable Acceleration Criteria (Tony Jumping) 53
Figure 4-17: Undamped SDOF System Coupled with a Damped Tuned Mass Damper 56
Figure 4-18: H_1' versus ρ 58
Figure 4-19: Sample Optimal Plot; Mass Ratio = 0.03, Frequency = 0.985 Hz. 59
Figure 4-20: H_1' versus ρ for optimal frequency and optimal damping ratio. (Altered from Connor, 238) 60

Figure 4-21 H_1' versus $\bar{m}$ 61

Figure 4-22: f_{opt} versus $\bar{m}$ 61

Figure 4-23 $\xi_{d\,opt}$ versus $\bar{m}$ 62

Figure 4-24: ξ_e versus $\bar{m}$ 62

Figure 4-25: Schematic of Single Joist with TMD attached, NTS (Portions from Connor, 233). 65

1. Introduction and Scope

With the growing demand for open, column-free floor spaces and the advances in material strength, floor vibration serviceability criterion has been of growing importance within the past 20-30 years. This aspect of structural design could simply be overlooked in the past for two specific reasons. The first reason is that the very small amplitude of these vibrations allows them to be ignored as a detriment to structural integrity. Secondly, these small vibrations would "die" out very quickly due to the larger damping and mass associated with the heavier structural system and dead load within the structure. (Murray 1979, ACC) In office buildings, for example, the floor-to-ceiling partitions, which provide additional support and damping to the floor system, have been replaced with cubicles. Additionally, the higher strength lightweight materials have significantly reduced the required cross-sections and, consequently, the stiffness of the structural materials. (Hanagan 2003, 3)

All floor systems are flexible and when introduced to a dynamic loading respond in a vibratory manner. The issues with floor serviceability arise when the floor vibrates in an uncomfortable way when exposed to everyday loading, for example human footfall in an office building. Although the very small vibrations do not affect the structural integrity or overall safety of the building, a person experiencing uncomfortable and very noticeable vibrations may not agree. Vibrating floors, therefore, have been divided into 4 categories: (a) vibration, though present, is not perceived by the occupants; (b) vibration is perceived but it does not annoy the occupant; (c) vibration annoys and disturbs; (d) vibration is so severe that it makes people sick. A design is considered successful if the floor falls into categories (a) and (b). Numerous studies have been conducted in order to quantify the acceptability criteria of the human response, the results of which will be later presented. (Galambos, 3)

This thesis is focused on the control of human induced floor vibrations. In order to provide the reader with practical insight on the subject, a case study of an existing steel framed office building that had experienced excessive and annoying floor vibrations will be discussed and analyzed. The study will explore the initial vibration issues that were experienced by the composite concrete slab and steel joist floor system, the consequent retrofit that was installed, the current status of the structure, an alternative retrofit solution, and future recommendations. Prior to the case study, the thesis will provide the reader with information on the basic principles of structural dynamics, the nature of the human induced loading, and, finally, an overview of the existing acceptable human response criteria and design guidelines.

2. The Nature of Human Induced Vibration

When a dynamic loading is applied to a structural system, the system responds depending of the type of dynamic loading. The following sections, 2.1 Basic Principles of Structural Dynamics and 2.2 Properties of Continuous Beams, will explain the basic principles of structural dynamics to give an understanding of how structures react to arbitrary dynamic loadings. The different types of dynamic loadings will be presented in 2.3 Dynamic Loading. An in-depth look at the response to periodic excitation will be exhibited in 2.4 Response to Periodic Excitation Following this, the dynamic loading of concern, human induced loading, and consequent response will be discussed in 2.5 Human Induced Loading and the Consequent Response.

2.1. Basic Principles of Structural Dynamics

When a structure is disturbed from its equilibrium position, it responds is a vibratory manner. A single degree of freedom (SDOF), shown in Figure 2-1, can be used as a simple model to explain the dynamic behavior of a structure.

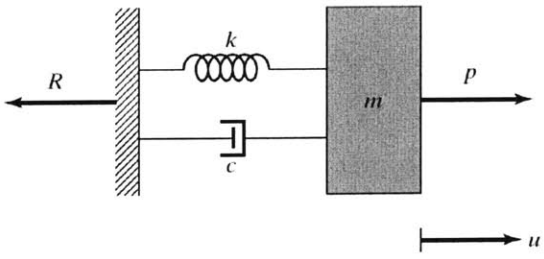

Figure 2-1: Single Degree of Freedom System (Connor, 9)

Using Newton's Laws of Motion the governing equation of motion for SDOF system is as follows:

$$m\ddot{u}(t) + c\dot{u}(t) + ku(t) = p(t) \quad \textbf{(2-1)}$$

where m, c, and k are the mass, viscous damping and stiffness properties of the system, respectively; u is the displacement; p is the periodic loading function; and t is the time. The dot indicates a derivative of displacement with respect to time; the first derivative, $\dot{u}$, being velocity and the second derivative, $\ddot{u}$, being acceleration. (Connor, 9-10)

From the above equation of motion, certain dynamic properties can be calculated. The natural frequency of a system is the measure of the frequency at which a body will vibrate during a state of vibration termed free vibration. Free vibration occurs when the body is simply displaced, released, and allowed to vibrate. The forcing function, *p(t)*, is equal to 0 during free vibration. The natural frequency of vibration of a system depends only on the mass and stiffness of the structure. The natural cyclic frequency of vibration, f_n, is a measure in hertz (Hz) of the number of vibrations, or cycles, that the structure experiences per second of free vibration. This is determined as follows:

$$f_n = \frac{1}{2\pi}\sqrt{\frac{k}{m}} \text{ [Hz]} \quad \textbf{(2-2)}$$

The natural circular frequency of vibration, ω_n, is measured in radians per second and can be calculated as follows:

$$\omega_n = \sqrt{\frac{k}{m}} = 2\pi \times f_n \text{ [Rad/sec]} \quad \textbf{(2-3)}$$

Both of these frequencies, f_n and ω_n, are termed the fundamental/natural frequency of vibration. (Chopra, 41)

Structures have many natural frequencies that are dependent upon the mode of vibration that is being experienced. As a structure is vibrating it moves with certain configurations which are termed mode shapes. The lowest frequency corresponds to the first mode of vibration. The

vibrating body has different modal properties which causes this change in frequency. In general, higher mode shapes have greater frequencies of vibration. Examples of typical beam and floor mode shapes can be seen in Figure 2-2 that follows. (Murray et al., 4)

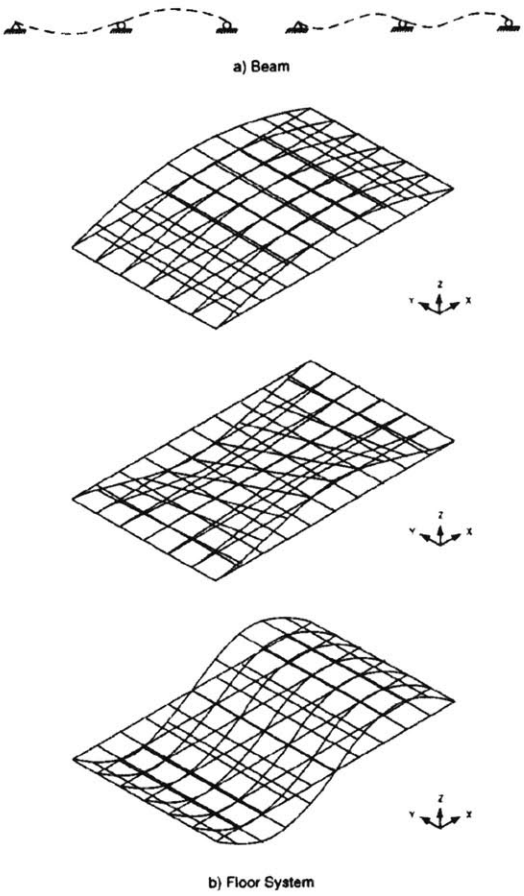

Figure 2-2: Typical a.) Beam and b.) Floor System Mode Shapes (Murray et al., 3)

The presence of damping in a system does have an effect on the overall response. Figure 2-3 represents a system experiencing free vibration, i.e. the forcing function $p(t)$ is equal to 0, which is free of damping. Notice the peak amplitude of displacement, indicated on the axis labeled "u", is constant and has a value of u_o. (Chopra, 40)

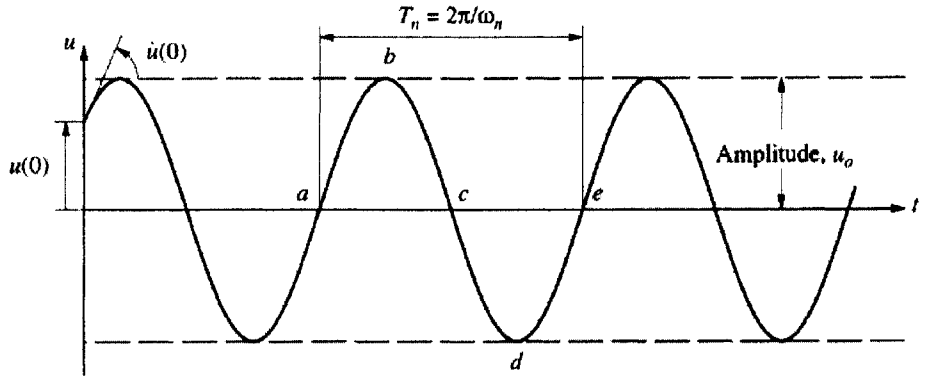

Figure 2-3: Free Vibration of a System without Damping (Chopra, p. 40)

In Figure 2-4, the free vibration response with damping has been added to the free vibration response without damping. It can be seen that the amplitude of displacement decays with the presence of damping. (Chopra, 50)

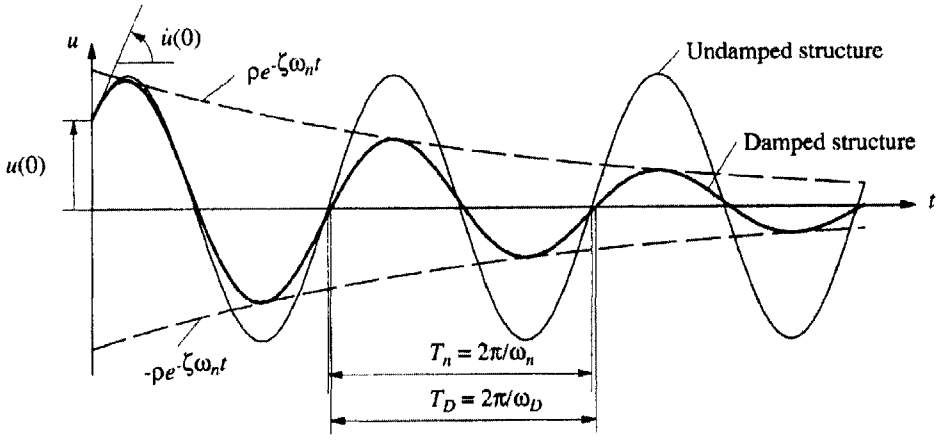

Figure 2-4: Effects of Damping on Free Vibration (Chopra, p. 50)

Also note from Figure 2-4 that the amount by which the amplitude decays over time is a function of the critical damping ratio, ξ. An example of this can be seen in Figure 2-5 below as the free vibration response is plotted with differing values of ξ.

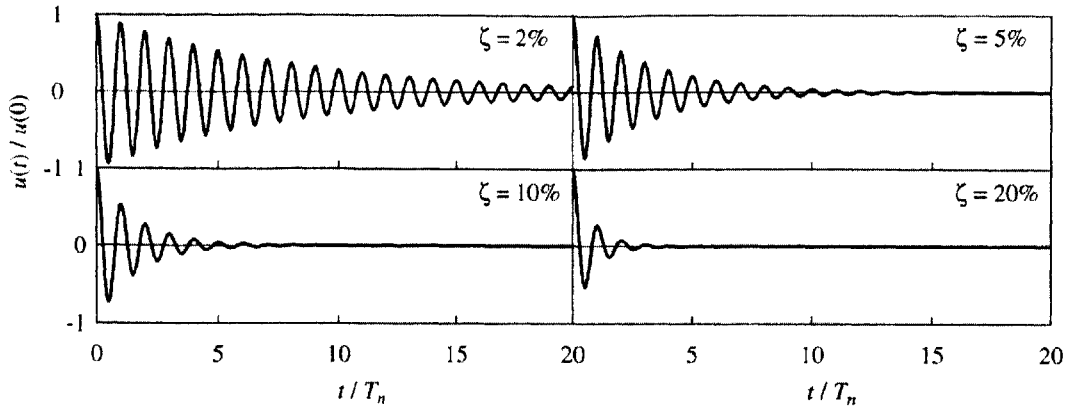

Figure 2-5: Free Vibration Response with Different Levels of Damping (Chopra, 51)

The critical damping ratio is a ratio of the actual damping constant, c, and the critical damping coefficient, c_{cr}:

$$\xi = \frac{c}{c_{cr}} \quad \textbf{(2-4)}$$

The critical damping coefficient is the smallest value of c that inhibits oscillation. Hence, as ξ is increased, the amount of time it takes for the free vibration to decay decreases. A structure is considered underdamped if the damping ratio is less than 1, critically damped if the damping ratio is equal to 1, and overdamped if the damping ratio is greater than 1. An underdamped structure will vibrate about its equilibrium position when excited with the amplitude of response decreasing over time. A critically damped structure will not oscillate and will return to its equilibrium position. Like the critically damped case, an overdamped structure will not oscillate, but it will take an infinite amount of time for the structure to return to its equilibrium position. An actual free vibration plot of an underdamped, critically damped, and overdamped system can be seen in Figure 2-6 below. For most structures of interest, i.e. buildings, bridges, etc., the critical damping ratio is typically below 0.1 and are, therefore, considered underdamped. (Chopra, 48-49)

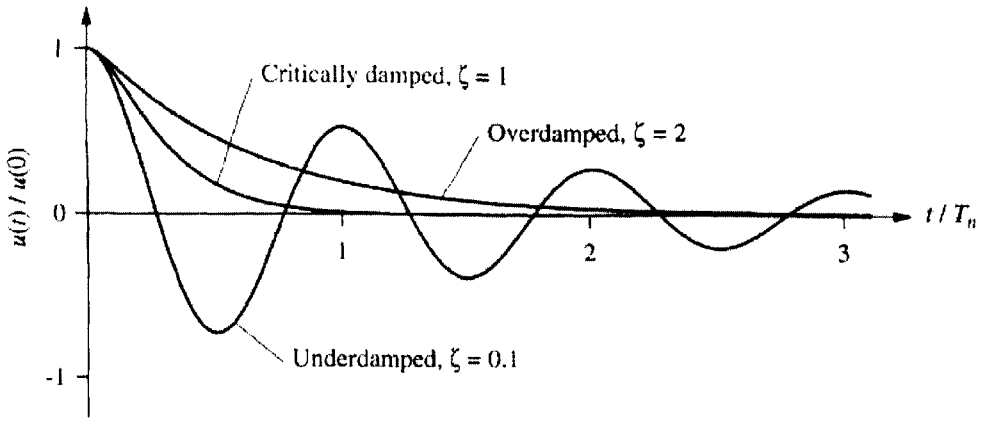

Figure 2-6: Free Vibration of Underdamped, Critically Damped, and Overdamped Systems (Chopra, 49)

The critical damping ratio can now be related to the damping coefficient, *c*, from the equation of motion through the following:

$$c = 2\xi\omega m = 2\xi\sqrt{km} \quad \textbf{(2-5)}$$

2.2. Properties of Continuous Beams

The basic principles can now be applied to more complex systems. The system considered in this study is a uniform simply supported continuous beam with mass, m, modulus of elasticity, E, and moment of inertia, I. As stated previously, there are different frequencies associated with the different modes of a system. The frequencies and corresponding mode shapes can be seen in Figure 2-7.

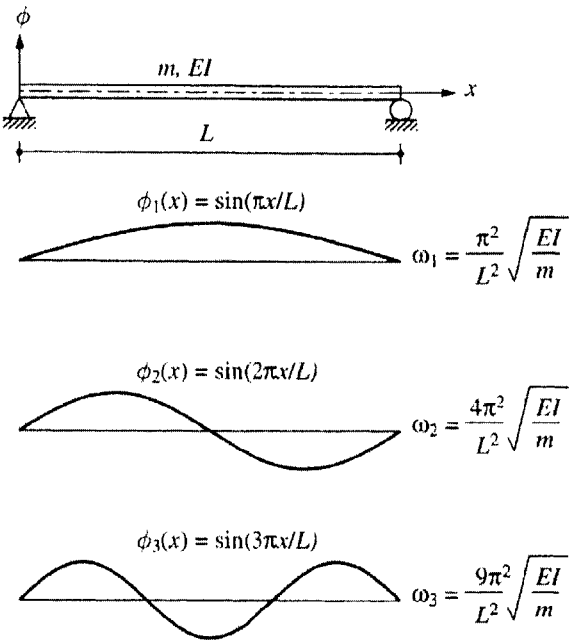

Figure 2-7: Natural Vibration Modes and Frequencies of Uniform Simply Supported Beams (Chopra, 635)

Also associated with each mode are the different modal properties, i.e. modal mass and modal stiffness. The modal mass and modal stiffness of a continuous uniform simply supported beam can be calculated as follows

$$\tilde{m}_j = \frac{L\rho_m}{2} \qquad \textbf{(2-6)}$$

$$\tilde{k}_j = EI\left(\frac{j\pi}{L}\right)^4 \frac{L}{2} \qquad \textbf{(2-7)}$$

where L is the length of the beam, ρ_m is the mass per unit length, and j the mode number. As you can see from these equations, the modal mass is not dependent on the mode number. (Connor, 267)

2.3.Dynamic Loading

In the previous sections there was no mention of the periodic loading, *p(t)*. Dynamic loadings can be categorized in 4 groups: harmonic, periodic, transient, or impulsive. Figure 2-8 displays some sample plots of the four loading functions versus time.

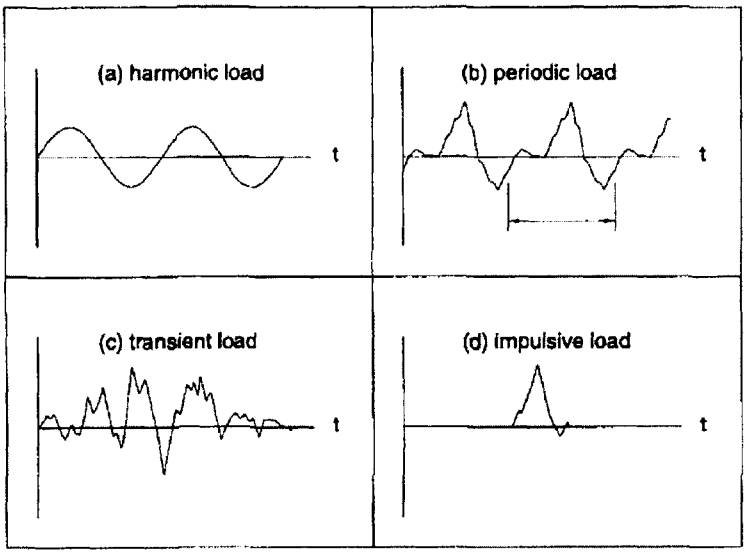

Figure 2-8: Types of Dynamic Loading (Murray et al., 2)

Harmonic loading varies according to a sine function and is generally caused by machines with out of balance forces. Periodic loading occurs when an arbitrary loading function is repeatedly applied over set intervals, or periods. This type of loading can be caused by rhythmic human motion, e.g. walking, aerobics and dancing, or by machines with more than one unbalanced mass, oscillating parts, or periodically impacting parts. Both harmonic and periodic loading are applied to and affect the structure for a long enough period of time such that the structure will respond in steady-state vibration. (Bachmann, 3)

Transient loading is a loading of arbitrary magnitude and time variation. There is no set period to the loading. This type of loading can be caused by human motion, earthquakes, water waves, and construction works. Impulsive loads, like transient loads, is of very short duration

and act as an impact. This type of loading can be caused by single jumps, heel-drop impacts, or any other impact with the load bearing surface. (Bachmann, 4)

All of the aforementioned types of loading have some effect on the structure that it is being applied to, the people that inhabit the structure, and/or the machines that are installed in or on the structure. Dynamic loading can affect both the structural integrity and the serviceability of a structure. For instance, fatigue, local plastification, and alteration of material properties can occur under certain loading conditions. Excessive motion can also damage nonstructural elements of the structure such as gypsum board walls or glass cladding. As vibrations occur in a structure a major serviceability issue is how the vibrations affect the humans that occupy them. Sensitive machinery, i.e. microscopes or other types of manufacturing machines, can also be affected by the secondary vibrations that transfer through the structure. (Bachmann, 5-6)

2.4.Response to Periodic Excitation

Taking $p(t)$, in equation as a sinusoidal forcing function with forcing frequency Ω,

$$p(t) = \hat{p}\sin(\Omega t) \quad \textbf{(2-8)}$$

where $\hat{p}$ is the magnitude of the force applied, the corresponding vibration response is given by,

$$u(t) = \hat{u}\sin(\Omega t - \delta) \quad \textbf{(2-9)}$$

where $\hat{u}$ is the maximum amplitude of displacement and δ is the phase angle shift of the response. The value of the maximum displacement is related to the magnitude of force, the stiffness of the system, and a dynamic amplification factor, H_1, in the following equation:

$$\hat{u} = \frac{\hat{p}}{k} H_1 \quad \textbf{(2-10)}$$

where the following equations define the transfer function H_1:

$$H_1 = \frac{1}{\sqrt{1-\rho^2]^2 + [2\xi\rho]^2}} \quad \textbf{(2-11)}$$

$$\rho = \frac{\Omega}{\omega} \quad \textbf{(2-12)}$$

$$\omega = \sqrt{\frac{k}{m}} \quad \textbf{(2-13)}$$

$$\xi = \frac{c}{2\omega m} \quad \textbf{(2-14)}$$

With equation (2-11) above, it can be noted that as the frequency ratio, ρ, approaches 1 the value of H_1 approaches infinity, assuming no damping in the system. This indicates that when the forcing frequency is equal to the natural frequency the amplitude of the response is infinite. This is termed resonance. A plot of the H_1 function versus the frequency ratio can be seen in Figure 2-9 below. It can be observed that when in the resonant frequency range damping has a strong influence on the amplitude of H_1 as the damping ratio, ξ, is the only remaining variable in the denominator of equation (2-11) when the frequency ratio is equal to unity. Outside the resonant frequency range the damping has little effect on the system response.

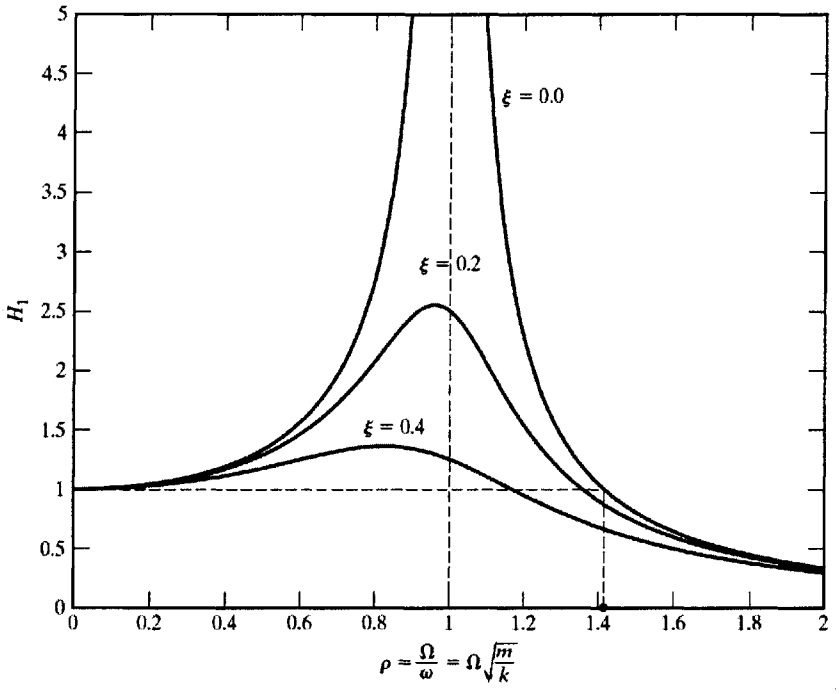

Figure 2-9: Plot of H_1 versus Frequency Ratio, ρ, and Damping Ratio, ξ (Connor, 11)

A similar dynamic amplification factor, H_2, can be developed for the system acceleration. H_2 is the amplification of u in terms of the acceleration. Differentiating the response, $u(t)$, with respect to time the acceleration, $a(t)$, is as follows:

$$a(t) = -\hat{a}\sin(\Omega t - \delta) \quad \textbf{(2-15)}$$

where,

$$\hat{a} = \frac{\hat{p}}{k}\Omega^2 H_1 = \frac{\hat{p}}{m}H_2 \quad \textbf{(2-16)}$$

$$H_2 = \rho^2 H_1 = \sqrt{\frac{\rho^4}{[1-\rho^2]^2 + [2\xi\rho]^2}} \quad \textbf{(2-17)}$$

The corresponding plot for the H_2 function can be seen in Figure 2-10. Notice the general similarities that exist between Figure 2-9 and Figure 2-10 with respect to the resonant excitation and the region which can be controlled with damping. (Connor, 11)

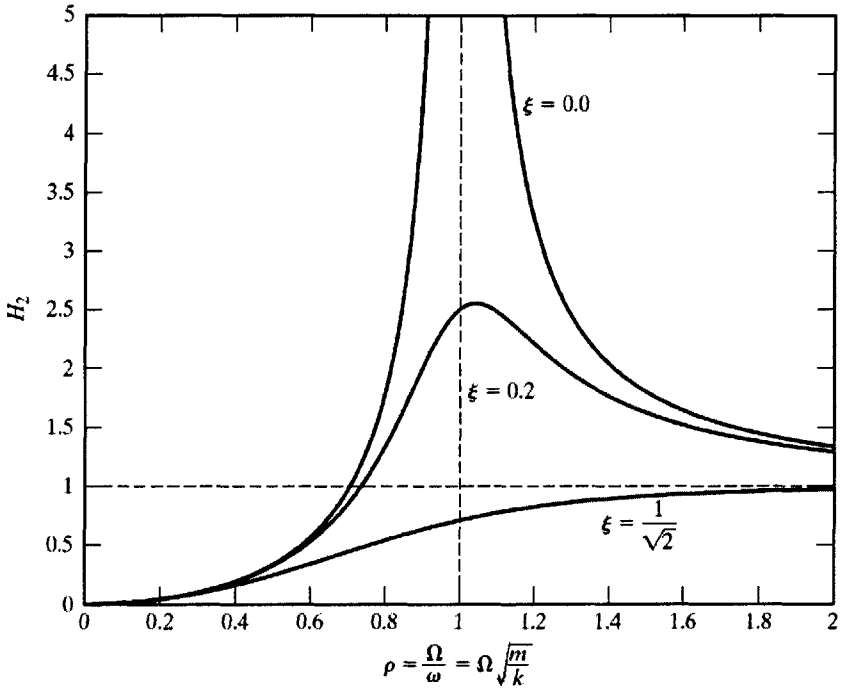

Figure 2-10: Plot of H_2 versus Frequency Ratio, ρ, and Damping Ratio, ξ (Connor, 13)

The figures shown above for H_1 and H_2 can be used as design charts when given certain system performance constraints (Design Example Adapted from Connor, 14-16). For instance, a system of mass, m, is constrained to a maximum acceleration value, a^*, for a specific loading, $\hat{p}$, a design amplification factor, H_2^*, can then be defined by the following:

$$H_2 \leq H_2^* = \frac{a^*}{\hat{p}/m} \quad \textbf{(2-18)}$$

Say, for example, an acceleration criteria of a system has been defined and $H_2^* = 2$. Figure 2-11 below indicates the values of H_2 that would satisfy the design requirement, which is

simply any value below the calculated H_2* value. As seen in the figure, H_2* for a particular damping ratio, ξ*, has two corresponding frequency ratio values, ρ_1 and ρ_2. In order to satisfy the given constraint the following must be true:

$$0 < \rho \leq \rho_1[H_2^*, \xi^*] \quad \textbf{(2-19)}$$

$$\rho \geq \rho_2[H_2^*, \xi^*] \quad \textbf{(2-20)}$$

When H_2* < 1 only equation (2-18) is applicable. For a given H_2* and ξ* the values of $\rho_{1,2}$ can be calculated with the following:

$$\rho_{1,2} = \sqrt{\frac{1 - 2\xi^{*2} \mp \sqrt{\left[1 - 2\xi^{*2}\right]^2 - 1 + \left[\frac{1}{H_2^*}\right]}}{1 - \left[\frac{1}{H_2^*}\right]^2}} \quad \textbf{(2-21)}$$

When there is no damping present in the system, $\rho_{1,2}$ can be determined with the following:

$$\rho_{1,2} = \sqrt{\frac{1}{1 \pm \frac{1}{H_2^*}}} \quad \textbf{(2-22)}$$

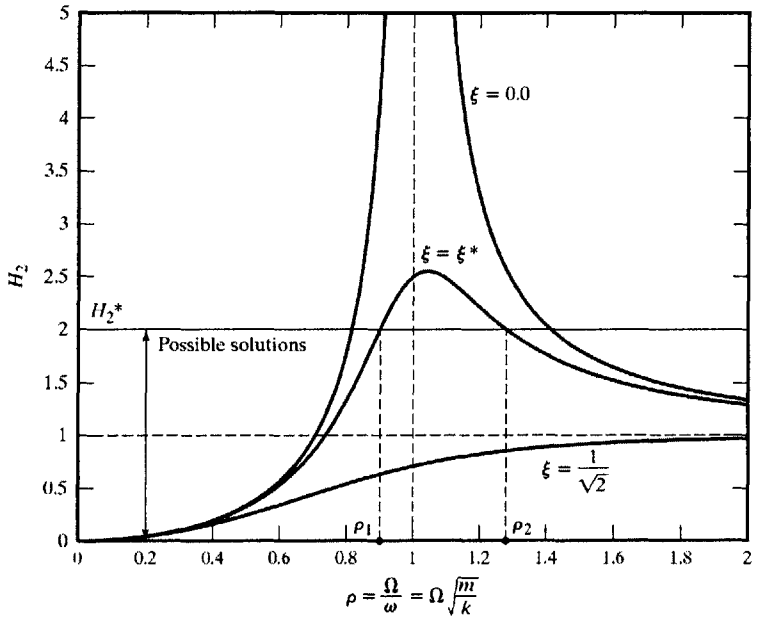

Figure 2-11: Acceleration Controlled Design Example

The limiting stiffness parameters can now be determined with the following:

$$k = \frac{\Omega^2 m}{\rho^2} \quad \textbf{(2-23)}$$

Notice for H_2*<1 there will only be one calculated value of k (corresponding to the one value of ρ) which will be the lower limit of the required stiffness. For H_2*>1 there will be two values of k, k_1 and k_2, corresponding to ρ_1 and ρ_2. The selected value of k must fall within one of the following ranges in order to satisfy the design constraint:

$$0 < k < k_2 \quad \textbf{(2-24)}$$

$$k_1 < k < \infty \quad \textbf{(2-25)}$$

Finally, with the damping ratio of the system, ξ^*, the mass of the system, m, and the stiffness parameter of the system, k, the damping parameter of the system, c, can now be determine from the following:

$$c = 2\xi\omega m = 2\xi\sqrt{km} \quad \textbf{(2-26)}$$

2.5.Human Induced Loading and the Consequent Response

Of primary importance in this study is the human-induced loading on floor systems and the consequent response. The effect of this vibration on humans the acceptable limits based on human comfort will be discussed in the section that follows. Human-induced loading can be extremely complex when dealing with both the lateral and vertical loading with each step. Both the lateral and vertical loadings are important considerations during design, for example, the London Millennium footbridge swayed excessively due to the lateral loading applied when a crowd walked across it. For the purposes of this study only the vertical loading of human footfall will be discussed as they are primary importance when dealing with floor systems. (Smith, 286)

Dynamic loading caused by humans generally occurs during motion such as walking, running, skipping or dancing. The forcing frequencies, typically denoted as f_s, at which these dynamic loads are applied to the structure vary from each case of motion. Typical forcing frequencies, f_s, forward speed, v_s, and stride lengths, l_s, can be found in Table 2-1 below.

Table 2-1: Common Forcing Frequencies, Forward Speed, and Stride Lengths (Bachmann, 15)

	f_s [Hz]	v_s [m/s]	l_s [m]
slow walk	~ 1.7	1.1	0.60
normal walk	~ 2.0	1.5	0.75
fast walk	~ 2.3	2.2	1.00
slow running (jog)	~ 2.5	3.3	1.30
fast running (sprint)	> 3.2	5.5	1.75

The actual nature of the human footfall loading can be seen graphically in Figure 2-12 below. The actual force-time curve tracks the loading cause by each step. The first step/foot is indicated by the solid line and the second step/foot is indicated by the dashed line. The initial increase in force is caused by the heel hitting the ground surface. This is then followed by the

leg stiffening and allowing the remainder of the body to pass across, indicated by the small dip in the curve. Finally, there is the "toe-off" force as the toe pushes off, indicated by the second increase in the solid line curve. The intersection of the two curves indicates that both feet are in contact with the ground at once. Hence the two forces can be added together, the resulting curve of which is depicted in Figure 2-13 below.

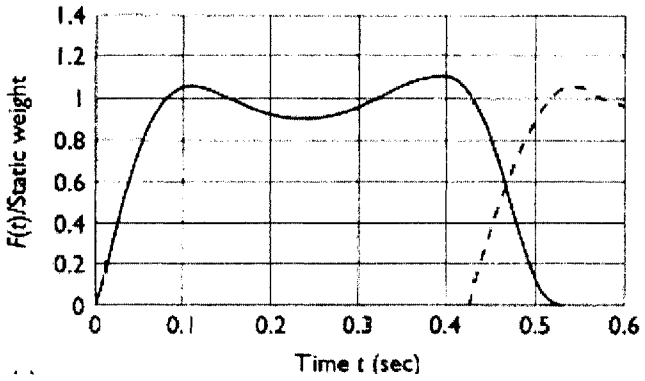

Figure 2-12: Force-Time Curves for Walking Body, Vertical Forces (Smith, 287)

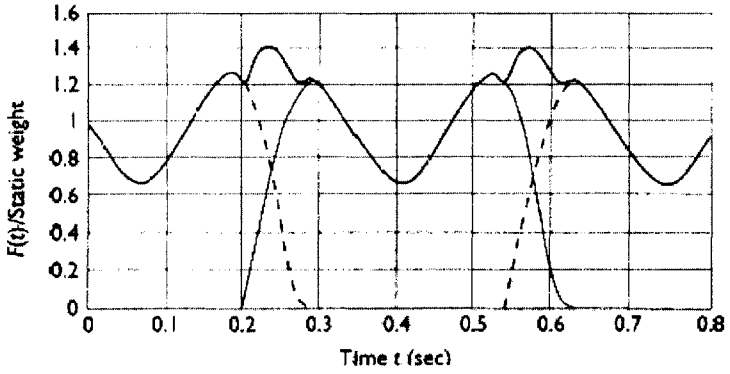

Figure 2-13: Force-Time Curves for Walking Body, Combined Vertical Forces (Smith, 287)

In cases where the floor spans are long, the above Figure 2-13 can be represented by a periodic forcing function. The forcing function can be represented as follows:

$$F = P[1 + \Sigma \alpha_i \cos(2\pi i f_{step} t + \phi_i)] \quad (2\text{-}27)$$

where P is the person's weight, α_i is the dynamic coefficient for the harmonic force, i is the harmonic multiple, f_{step} is the step frequency of the activity, t is the time, and ϕ_i is the phase angle for the given harmonic. Typical values of the above parameters for a person walking are listed in Table 2-2 below. (Murray et al., 3)

Table 2-2: Common Forcing Frequencies and Dynamic Coefficients (Murray et al., 8)

Harmonic *i*	Person Walking	
	f, Hz	α_i
1	1.6–2.2	0.5
2	3.2–4.4	0.2
3	4.8–6.6	0.1
4	6.4–8.8	0.05

As a floor is loaded by a walking person, there is a measurable response. A time-history plot shows the magnitude of the parameter being measured, for example, acceleration, versus time. A sample acceleration time-history plot taken from a study conducted by Hanagan et al. is depicted in Figure 2-14 below. Also depicted is the frequency spectrum. There are many observations that can be made from the plots. Firstly, the dominant frequency of the response can be determined and compared to the calculated values. Secondly, the actual magnitudes of the measured parameter, here acceleration, are depicted in the time history plot and can be compared to the recommended values. Thirdly, the type of response experienced by the floor can be determined and the type of loading can be deduced.

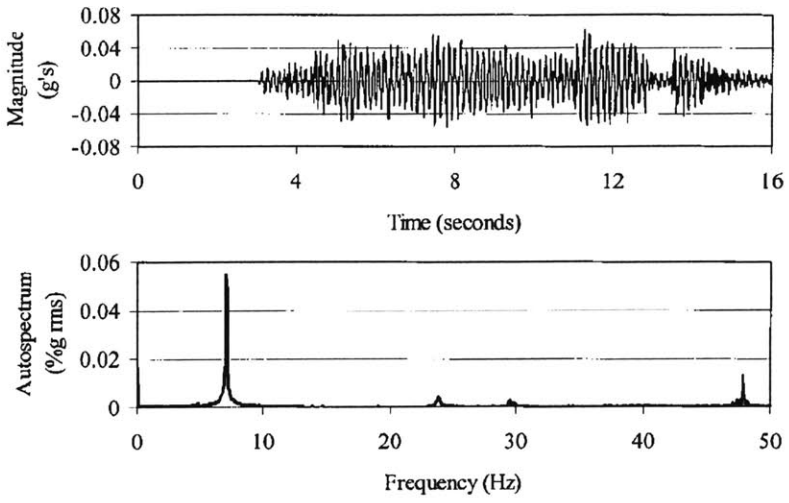

Figure 2-14: Sample Time History Plot and Frequency Spectrum (Hanagan et al., 128)

3. Design Aids and Suggestions

Studies concerning the acceptable human response criteria to vibratory motion have been conduction since early portion of the 20th century. These studies, which date back to the early 1930s, vary with the parameters measured, i.e. acceleration versus amplitude of displacement, and dynamic loading applied, i.e. steady state vibration versus vibration experienced due to transient loading. (Murray 1979, 68)

Studying the human response to vibration is rather difficult as it deals with the actual dynamic behavior of the human as a whole and it also deals with a non-physical aspect of the human anatomy: the psychology of the human. Hence, along with measuring the acceleration of the human body, it must also be documented how the human felt during the vibration experience. For example, the human response can be classified in to the following four groups:

(a) Vibration, though present, is not perceived by the occupants.

(b) Vibration is perceived but it does not annoy the occupant.

(c) Vibration annoys and disturbs.

(d) Vibration is so severe that it makes people sick.

Floor systems that fall into the first 2 categories are considered acceptable as the humans in the structure do not feel any discomfort. The last two categories may make the human feel unsafe in the structure or even feel uneasy. "Annoying levels of vibration, due to people walking, generally occur when a [harmonic] multiple of the walking pace is in resonance with the fundamental natural frequency of the floor system" (Hanagan et al., 127). Floor systems typically have fundamental natural frequencies of approximately 5-8 Hz. This is a rather important observation because the organs of the human body have natural frequencies that fall in

this range. Hence, the human walking load is exciting the floor at resonance, the floor, in turn, is exciting the human body in resonance. (Hanagan et al., 127)

This chapter will outline the previous studies that have been conducted to determine appropriate comfort levels for humans when exposed to vibration. The different studies attempted to base the human comfort level on different parameters, the most widely used human response scales of which will be discussed in 3.1 Human Response Criteria. A more comprehensive list of the acceptance criteria developments in chronological order viewed in Appendix A. The prominent design guide that deals with the forced vibration of steel beam and concrete slab floor systems will then be discussed in 3.2 Vibration Design Criteria for Steel Beam-Concrete Slab Construction.

3.1. Human Response Criteria

3.1.1. Modified Reiher and Meister Scale

In 1931, Reiher and Meister developed human response criteria. These criteria were developed by exposing a group of standing people to a steady-state vibration. The frequencies of these vibrations ranged from 5 to 100 Hz with amplitudes ranging from 0.01 mm (0.0004 in.) to 10 mm (0.4 in.). As the people experienced these vibrations, the perceptibility level was then noted in ranges from "barely perceptible" to "intolerable". (Murray et al., 67) Following this development, Lenzen (1966) further applied the Reiher-Meister scale to steel joist-concrete slab office floors. Rather than exposing test subjects to a steady-state vibration, Lenzen used a single impact to excite the floor and then determined the human perceptibility. The ultimate conclusion of his study was that the original scale was suitable for floors with less than 5 percent critical

damping if the amplitude was increased by a factor of 10. A plot of the Modified Reiher-Meister Scale can be seen in Figure 3-1 below.

In 1974 and 1975, McCormick and Murray, respectively, utilized this scale to develop design criteria for office floors. Their contributions to the Modified Reiher-Meister Scale can also be seen in Figure 3-1 below. McCormick suggested that floors with damping less than 3% that plot below "Line B" in the figure below to be acceptable, although everyday human walking excitation may be perceived by the occupants. Murray suggested that "systems with 4% to 10% critical damping which 'plot above the upper one-half of the distinctly perceptible range will result in complaints from occupants; and systems in the strongly perceptible range will be unacceptable to both occupants and owners' " (Murray, 64). Murray's suggestion for heel-drop loading can be seen marked as "Line A" in the figure below. (Murray, 64)

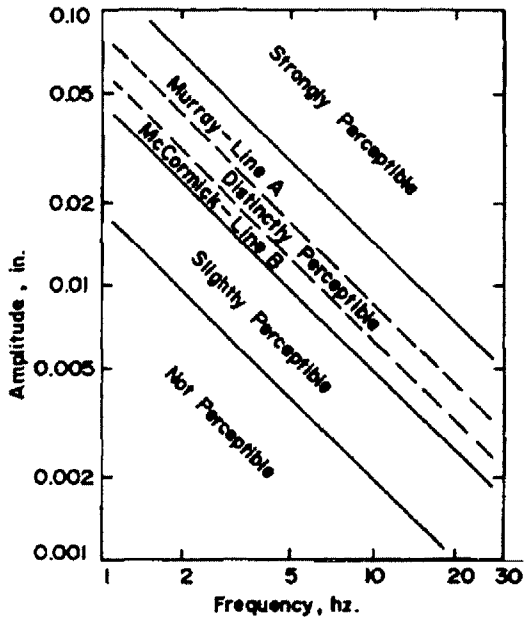

Figure 3-1: Modified Reiher-Meister Scale (Murray, 63)

3.1.2. Wiss and Parmelee

In 1974, Wiss and Parmelee exposed 40 humans to a vibratory force that was similar to that caused by a human footfall. The parameters that were varied in the experiment included frequency, amplitude, and damping. As a result of the testing and some statistical analysis of a subjective numerical rating of the vibration experienced, the following human response criteria formula was developed:

$$R = 5.08\left[\frac{fA_o}{D^{0.217}}\right]^{0.265} \quad \textbf{(3-1)}$$

where R is the mean response rating, which is based on a numerical scale with the following numerical designations:

$R=1$ imperceptible vibration,

$R=2$ barely perceptible vibration,

$R=3$ distinctly perceptible,

$R=4$ strongly perceptible,

$R=5$ severe vibration,

f is the frequency, A_0 the maximum amplitude, and D the damping ratio. (Murray, 83)

The Wiss and Parmelee scale has been plotted in comparison with the Modified Reiher-Meister scale and can be seen in Figure 3-2.

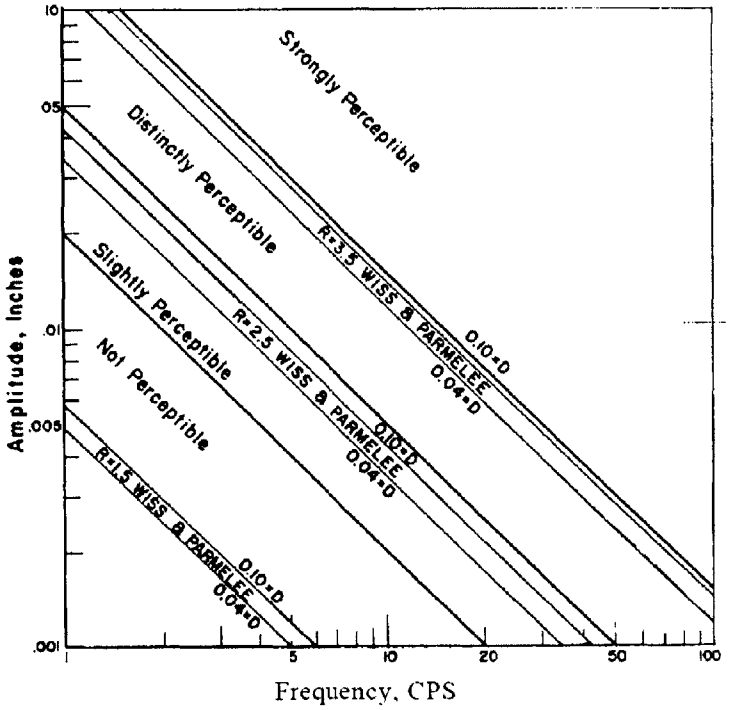

Figure 3-2: Comparison of Modified Reiher-Meister and Wiss-Parmelee scales (Murray, 83)

3.1.3. Canadian Standards Association Scale

Allen and Rainer developed these criteria in 1976 by testing a series of long-span floor systems with a heel-drop load test. This type of test requires the measurement of the vibration response due to a human dropping his/her foot on the floor of concern. The office floor scale developed as a result of their study can be seen in Figure 3-3 below. The peak acceleration as a percent of gravity is a function of the frequency and damping. In the figure below, the following cases of vibration are plotted:

- Walking Vibration Continuous (10-30 Cycles)
- Walking Vibration Transient (3% Damping)
- Walking Vibration Transient (6% Damping)
- Walking Vibration Transient (12% Damping)

Ellingwood notes of the Allen and Rainer scale, "If the motion essentially damps out within approximately 5 to 10 cycles, the level of acceleration considered tolerable is higher by approximately a factor of 10 than if the excitation is continuous" (Ellingwood, 403)

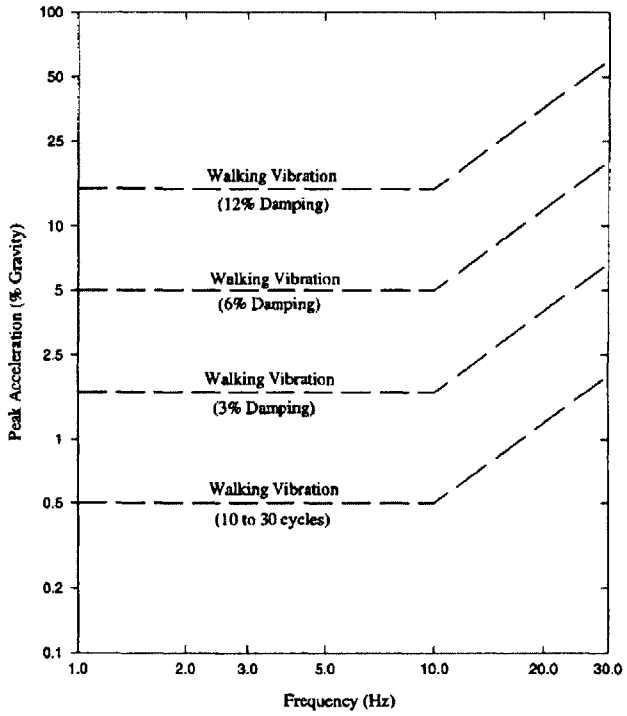

Figure 3-3: Canadian Standards Association Scale developed by Allen and Rainer (Murray et. al, 69)

3.1.4. Murray Criterion

In 1981, Murray performed a similar study as Wiss and Parmelee, with a heel-drop loading, and developed a design criterion. The criterion specified a damping requirement based on the same parameters, maximum amplitude and frequency, as Wiss and Paremelee in section 3.1.2 Wiss and Parmelee (Ebrahimpour, 2489). The suggested criterion is as follows:

$$D > 35A_0 f_n + 2.5 \quad \textbf{(3-2)}$$

where f_n is the frequency, A_0 the maximum amplitude, and D the damping ratio. (Murray, 68)

3.1.5. International Organization for Standardization Scale

The International Organization for Standardization's standard ISO 2631-2: 1989 contains many different human response criteria for numerous loading conditions. The ISO plot can be seen in Figure 3-4 below. A baseline curve of Peak Acceleration versus Frequency for transient loading was developed and, depending on the use of the structure, the peak acceleration is determined by an occupancy multiplier (Ebrahimpour, 2489). Hence, from the figure below it can be seen that a "shopping mall" occupancy would have a larger multiplier resulting in a larger acceptable acceleration limit.

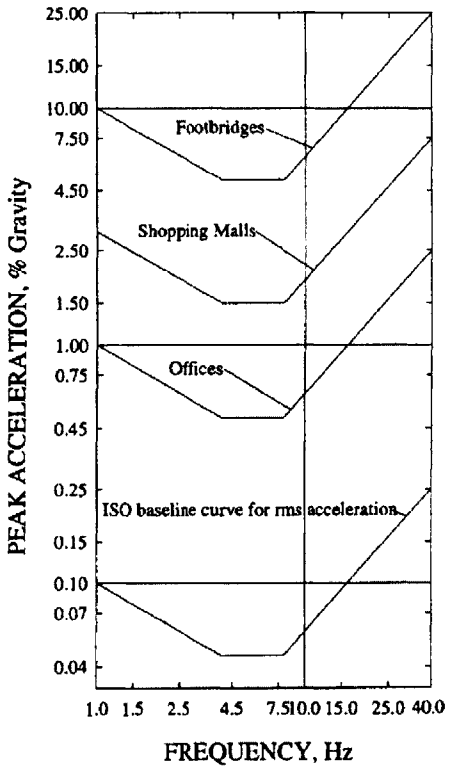

Figure 3-4: ISO Scale (Murray et al., 69)

3.2. Vibration Design Criteria for Steel Beam-Concrete Slab Construction

The most recently published and comprehensive vibration design guideline is a joint publication of the American and Canadian Institutes of Steel Construction entitled Floor

Vibrations Due to Human Activity (Steel Design Guide 11). The guide provides design criteria for walking excitation, rhythmic excitation and sensitive equipment. For walking excitation, the guide references ISO 2631-2: 1989(Figure 3-4 above) as the acceptable acceleration limits. The actual peak acceleration as a percent of gravity, which is not to exceed the aforementioned limits, is determined by the following:

$$\frac{a_p}{g} = \frac{P_0 \exp(-0.35 f_n)}{\beta W} \quad \text{(3-3)}$$

where P_0 is a constant force representing the excitation, f_n is the natural frequency of a beam or joist panel, a girder panel, or a combined panel as applicable, β is the modal damping ratio, and W the effective weight supported by the beam or joist panel, girder panel of combined panel, as applicable. In Table 3-1 typical values for the parameters found in equation (3-3) above can be found for varying occupancy types.

Table 3-1: Recommended Values of Parameters in Equation (3-3)

	Constant Force P_o	**Damping Ratio β**	**Acceleration Limit $a_o / g \times 100\%$**
Offices, Residences, Churches	0.29 kN (65 lb)	0.02–0.05*	0.5%
Shopping Malls	0.29 kN (65 lb)	0.02	1.5%
Footbridges—Indoor	0.41 kN (92 lb)	0.01	1.5%
Footbridges—Outdoor	0.41 kN (92 lb)	0.01	5.0%

* 0.02 for floors with few non-structural components (ceilings, ducts, partitions, etc.) as can occur in open work areas and churches,
0.03 for floors with non-structural components and furnishings, but with only small demountable partitions, typical of many modular office areas,
0.05 for full height partitions between floors.

4. Floor Vibration Case Study: Bank in Massachusetts

In the sections that follow a case study of a two-storey building that experienced excessive, uncomfortable floor vibration is presented. The structure is a bank in Massachusetts, the name of which is to remain undisclosed at the branch manger's request and will hereinafter be referred to as "Bank". Section 4.1 provides background information about the structure, a general overview of the original vibration problem that was experienced, and a brief timeline of the testing and changes that occurred in the structure. Section 4.2 will outline the original structural assessment and retrofit scheme proposed and installed by a consultant structural engineer. Section 4.3 will present the current status of the floor system as determined by recent (2007) vibration testing. Section 4.4 will describe alternative methods that may be employed to control the vibration issue. Section 4.6 will provide conclusions and offer recommendations as suggested by the analytical results of this study.

4.1. Background Information and Introduction to Vibration Problem

In 1988, customers and bank personnel were experiencing rather uncomfortable floor vibrations in a recently added section of the building. These vibrations were so uncomfortable, that customers actually left in fear of their safety or because of the "sea-sickness" that they felt while sitting at a bank representative's desk. The branch manager, primarily concerned that the vibrations were unsafe and presumably upset with how the vibrations were affecting the operation of the Bank branch, contacted a structural engineer to assess the situation. An analysis was first conducted to determine if the structural system of the floor was safe for the given dead and live loads, which determined that the vibration was only a serviceability issue. Next, a dynamic analysis was conducted to determine the vibration characteristics of the structure. After

the analysis, suggestions to prevent the motion were presented to the client, eventually leading to the installation of a retrofit scheme that alleviated the vibration issue. The floor vibrations were much less noticeable after the retrofit installation. However, no vibration tests were conducted to verify the actual dynamic properties of the "new" system.

Between 1988 and 2007, there were noticeable changes in the office arrangement. For example, wall partitions, which are not connected to the second floor, were installed and file cabinets and additional desks were moved to the area of concern. After a recent interview with the branch manager, it was noted that the vibrations were, in fact, even less noticeable after the installation of the wall partitions and relocation of the furniture than they were after the original retrofit was installed. Testing was conducted on 23 April 2007 to determine the current dynamic properties, specifically the frequency of the system and acceleration of the vibrations that occurred when different types of human loading were applied.

4.2. Data Collection (1988 Testing), Analysis, and Consequent Retrofit

The following sections will discuss the previous study conducted by the consultant engineering while adding input where necessary. Section 4.2.1 presents the data collected in 1988, a comparison of the data collected and the theoretical values, and suggests a reason for the difference between the actual and theoretical values. Section 4.2.2 presents the retrofit scheme that was chosen and provides insight as to why this scheme was chosen.

4.2.1. Data Collection and Analysis

At the request of the structural engineer, the floor was put under a series of tests to determine the actual frequency of the floor system. In April of 1988, a vibration survey was conducted that measured impact and foot traffic responses in the area of the Bank floor that was

experiencing the annoying vibrations. Acceleration (vertical) time-histories were tape recorded using highly sensitive accelerometers. The actual instrumentation used was as follows:

- Wilcoxon Research Model100A Seismic Accelerometers (10 volts/g output, resonant frequencies= 925 Hz)
- Encore Electronics Model 502 Four Channel Instrumentation Amplifier
- TEAC Model R61-D Four Channel Analog Data Magnetic Tape Cassette Recorder (FM recording frequency DC to 625 and 50dB signal to noise ratio)
- Verbatim T-300H Data Cassette Tapes

The actual loading of the floor varied in order to record a representative sample. The tests tracked the response of the floor as 3 different sized people individually walked across the floor. An impulse response of the floor was obtained by dropping a 30 lb. weight from differing heights. The load cases are as follows:

- John (215 lbs) walking
- Tony (170 lbs) walking
- Sheila (120 lbs) walking
- 30 lb weight dropped from height of 2 ft.

The vibration amplitude data were then analyzed and plotted as acceleration amplitude versus frequency, frequency spectrum, to determine the frequencies that are present during the excitation. The following figures, Figure 4-1through Figure 4-3, display the acceleration time-histories and the relative acceleration amplitude versus frequency spectra as recorded for the three walking loads mentioned previously.

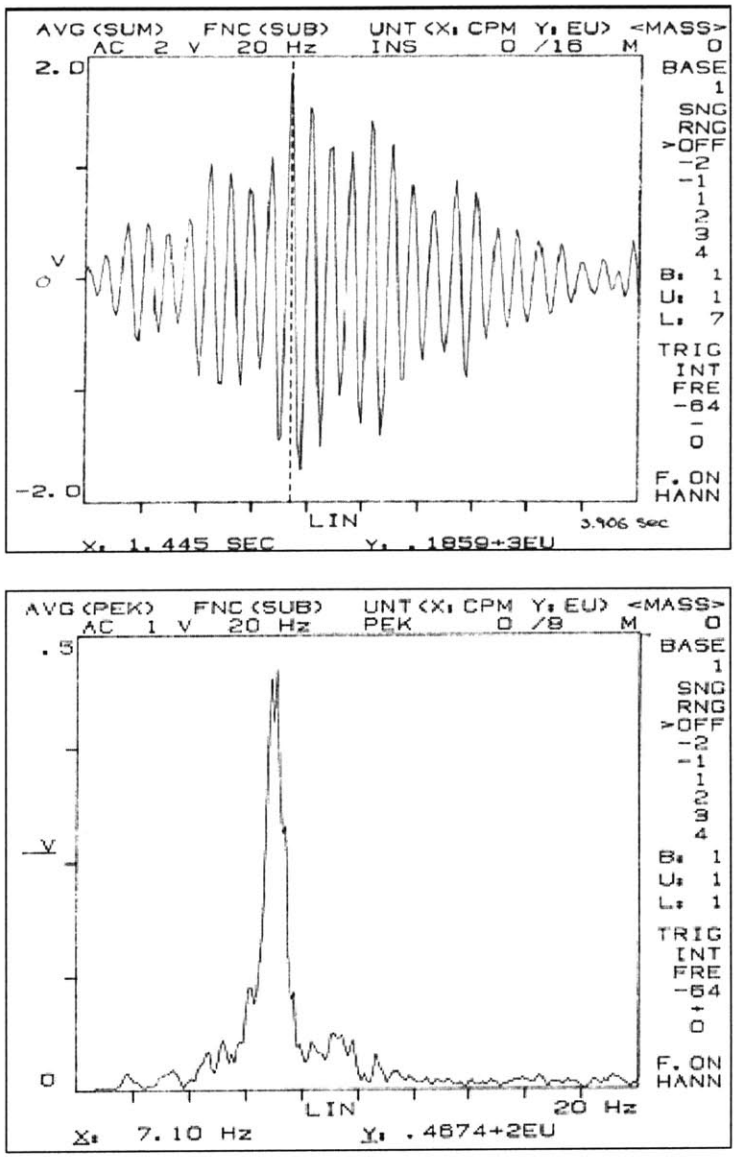

Figure 4-1: Acceleration Time-History and Frequency Spectrum (John walking)

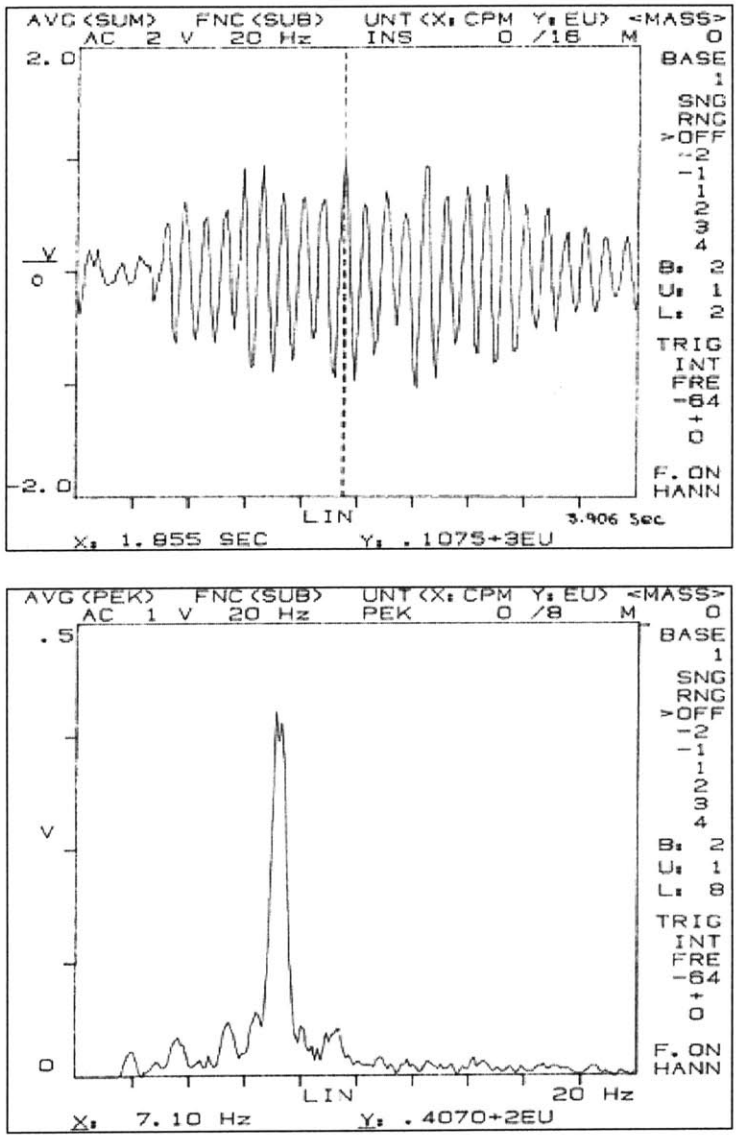

Figure 4-2: Acceleration Time-History and Frequency Spectrum (Tony walking)

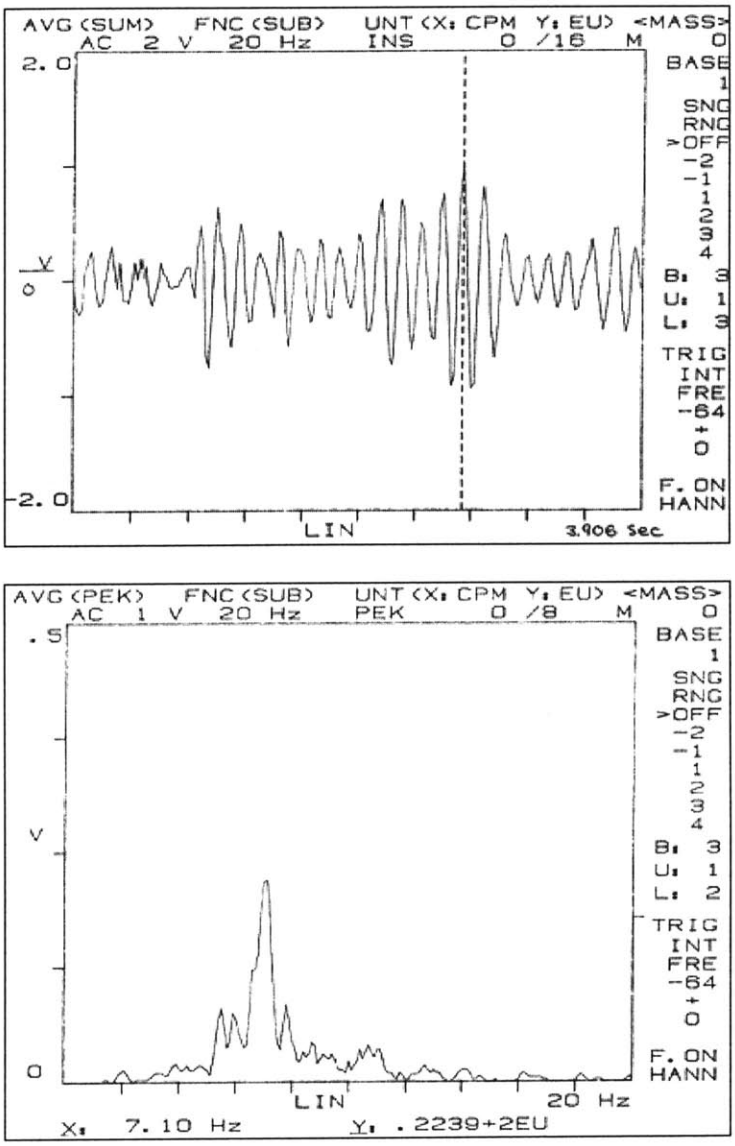

Figure 4-3: Acceleration Time-History and Frequency Spectrum (Sheila walking)

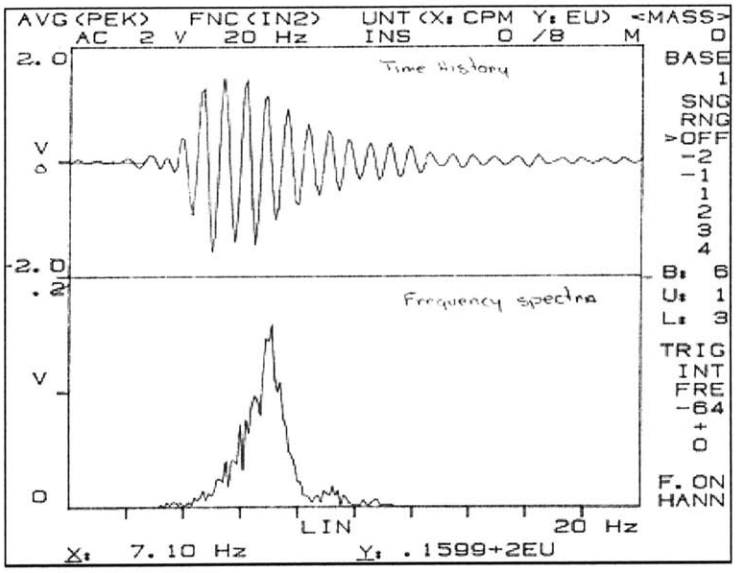

Figure 4-4: Acceleration Time-History and Frequency Spectrum (30 lb. dropped 2 ft.)

From the above figures it can be deduced that the natural frequency is approximately 7.10 Hz. for all three cases. The maximum acceleration amplitude of 2 m/s^2 was experienced when the floor was excited by the larger loading (John walking). It was also noted that as John walked across he floor, the vibrations were extremely uncomfortable to the people present during the testing. A summary of the maximum acceleration and corresponding displacement can be found in Table 4-1.

Table 4-1: Summary of Results from Past Testing

	Past Data		
	John Walking	Tony Walking	Sheila Walking
Measured Frequency (Hz)	7.1000	7.1000	7.1000
Maximum Acceleration (m/s^2)	2.0000	1.0000	0.7500
Maximum Acceleration (% g)	20.4%	10.2%	7.6%
Maximum Deflection (mm)	1.0050	0.5025	0.3769
Maximum Deflection (in)	0.0396	0.0198	0.0148

The floor system is composed of an open-web steel joist supporting metal deck and concrete. The overall span of the joists is 25.5 feet and they are spaced 2.5 feet on center. A picture of an existing joist and steel deck of the floor system can be seen in Figure 4-5.

Figure 4-5: Steel Joist and Metal Deck (Homem)

The natural frequency of the simply supported composite joist was calculated to be 10.65 Hz. This value is approximately 4.5 Hz. greater than the measured frequency. The natural frequency of the joist alone, including the mass of the concrete but neglecting the composite action acting between the two, was calculated to be 6.3 Hz. A summary of the findings can be found in Table 4-2 below.

Table 4-2: Calculated and Measured Frequencies

	Frequency [Hz]
Calculated Frequency (Composite)	10.65
Calculated Frequency (Non-Composite)	6.3
Measured Frequency	7.1

Hence, from this observation, it can be deduced that the joist and slab are not acting as a composite section. It was also observed on site that there was a small gap between the joist and

metal deck with only intermittent welds attaching the two. Ellingwood notes of previous studies have shown that, "Shear friction between joists and slab was found to be sufficient to cause composite action under small amplitude excitation" (Ellingwood, 407). This being the case, there is limited shear friction between the joist and metal deck/concrete slab that would cause the system to act compositely. It was later found out that the building was constructed during the winter and it was suggested that moisture may have frozen between the joist and deck during the concrete curing process.

4.2.2. Consequent Retrofit

There are different methods to solving dynamic problems that occur in structures. Since damping is very effective for systems in resonance with the loading function, damping could be added to the system. This can be done in numerous ways some examples of which include adding damping devices, floor to ceiling partitions, drop ceilings, or thick carpeting. Another method is to either adjust the frequency of the structural system or loading function such that the two frequencies are not in resonance with each other, essentially changing the frequency ratio from 1 to a value greater or less than 1. Since human walking is very similar from one person to the next, i.e. similar walking frequencies and force, it is necessary to adjust the system parameters. Revisiting equation (2-13) it can be seen that the natural frequency of a system is a function of the system mass and stiffness. Therefore, in order to change the natural frequency of the system, it is necessary to add either mass and/or stiffness to the system. Note it is possible to reduce mass and stiffness but in the case of an as-built structure it is difficult to do so. In the case were both mass and stiffness are added to the system, they must not be added in proportional amounts as the frequency will not change if they are added proportionately. (Connor)

The original suggestion made by the engineer was to increase damping by adding floor to ceiling partitions and new, thicker carpeting. Also suggested was the installation of a series of tuned masses, which were essentially assemblies consisting of a mass on a spring each tuned to the natural frequency of the floor.

This fix would require construction in the Bank and therefore, further business disruption. Another alternative to increase the stiffness of the system was sought by the engineer. The next proposal was to include a series of round rods that would be connect to the bottom of the floor joists and the concrete basement floor. The rods would be preloaded in compression to its buckling load as this would allow for an easier connection with the concrete floor and it would assure that the maximum amount of force the foundation would experience would be the buckling load. Rather than pretension the rods and have to install a tension connection with the concrete floor, the rods were preloaded in compression such that there was a slight "bow" or initial crookedness in the rods. As a person walks across the floor, the rods compress further and buckle elastically. As the floor vibrates, the rod goes through cycles of straightening out and elastic buckling. When the rod straightens out it impedes the vibration until the floor system returns to its static state, the dead load of which will bring the rods back to its buckled state.

A schematic depiction of this scheme can be found in Figure 4-6. This was achieved first by connecting the rods with the bottom of the steel joist as shown in Figure 4-7. The rods were slender enough that they could be bent slightly. The other end of the rod was then placed in small slot or circular groove that was drilled in the concrete, hence, the rod would be compressing against the concrete and steel joist. A series of these rods as-built can be seen in Figure 4-8. Following the installation of the preloaded rods, the vibrations were less annoying

and actually bearable by the employees and customers. Under certain conditions however, the vibrations were still felt.

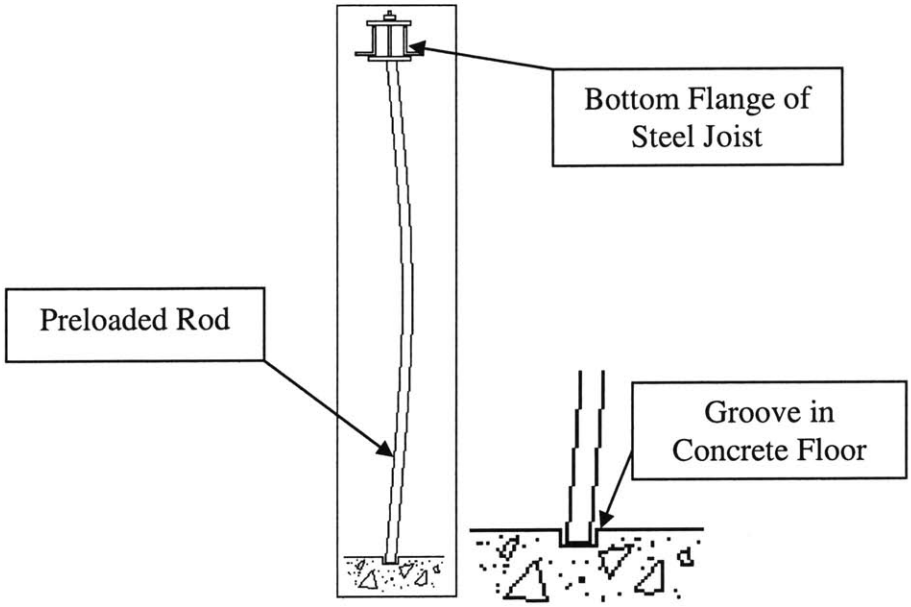

Figure 4-6: Schematic Drawing of Preloaded Slender Rod and Concrete Slot Detail

Figure 4-7: Rod Connection with Bottom Flange of Steel Joist (Homem)

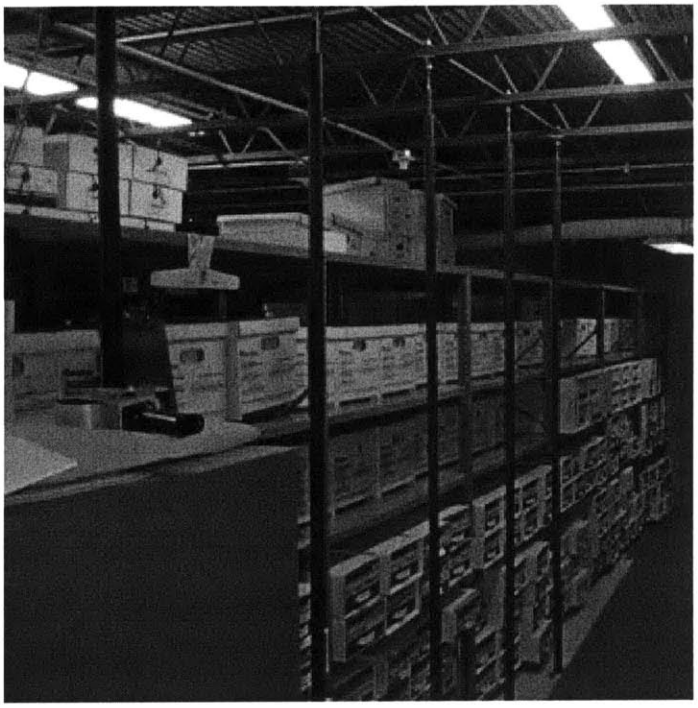

Figure 4-8: Series of Preloaded Rods (Homem)

4.3. Current Status of Floor System

Following the 1988 testing of the bank floor, no other testing was conducted to determine vibration characteristics after the retrofit was installed. Between 1988 and 2007, there were major modifications to the Bank. For example, there were permanent partitions installed, which can be seen in Figure 4-9, along with the addition of heavy file cabinets and desks. It was noted by the branch manager that following the addition of the partitions and desks the vibrations were less uncomfortable, but still noticeable under certain conditions. For example, after interviewing a current employer of the Bank, she said that she is still able tell who is coming to her desk by the vibration that she feels.

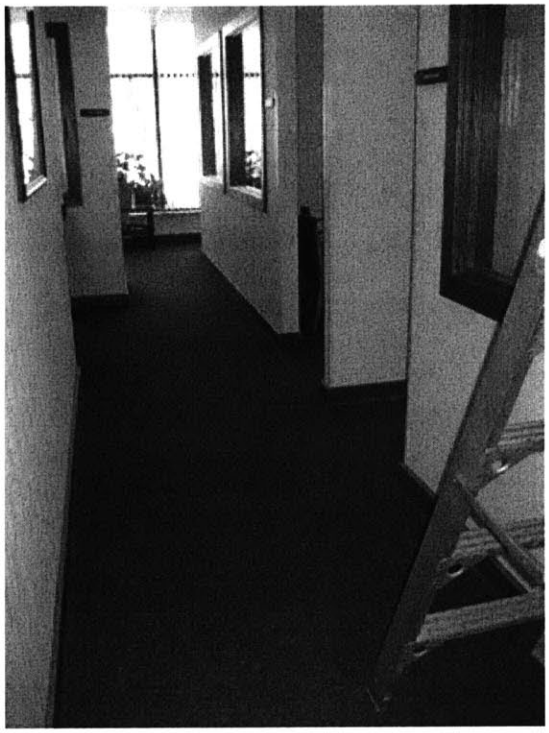

Figure 4-9: Floor with Vibration Issue and Partitions Added (Homem)

On 23 April 2007, similar tests were conducted on the same Bank floor span that experienced the vibration problems in the past. The actual testing apparatus used is as follows:

- Vernier Low-g Accelerometer (Figure 4-10 a.)
- Vernier LabPro Transfer Device (Figure 4-10 b.)
- Sony Vaio Laptop with Vernier LoggerPro 3 Software installed

a. b.

Figure 4-10: a.) Low-g Accelerometer b.) LabPro Transfer Device

The accelerometer was mounted on a desk where the vibrations are known to have been felt the most. The desk was located at the midpoint of the joist, essentially the center of the rectangular floor. The accelerometer was then connected to the LabPro Transfer device which then fed the readable data to the computer. Plots of the acceleration time-history were plotted in real time as the floor was loaded.

Acceleration time-histories and the corresponding frequency spectra were collected for a range of loading scenarios. Similar to the previous loading cases, the load cases were as follows:

- Colin walking heavily (200 lbs)
- Tony walking (170 lbs)
- Tony jumping/bouncing with a frequency close to the floor frequency (170 lbs)

The following figures, Figure 4-11 through Figure 4-13, exhibit the acceleration time-history and the relative acceleration amplitude versus frequency spectra for the above load cases.

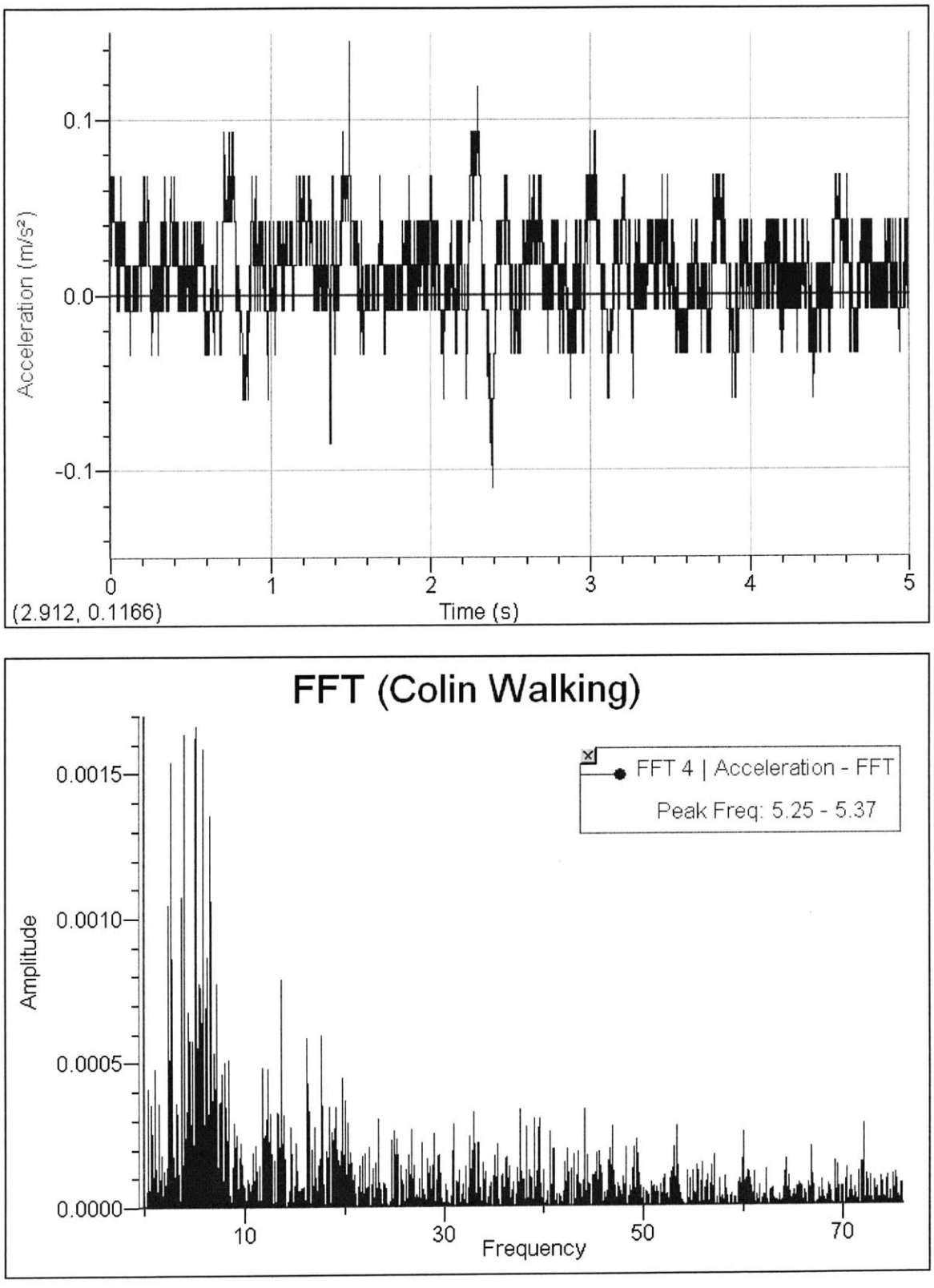

Figure 4-11: Acceleration Time-History (above) and Frequency Spectrum (below) (Colin Walking Heavily)

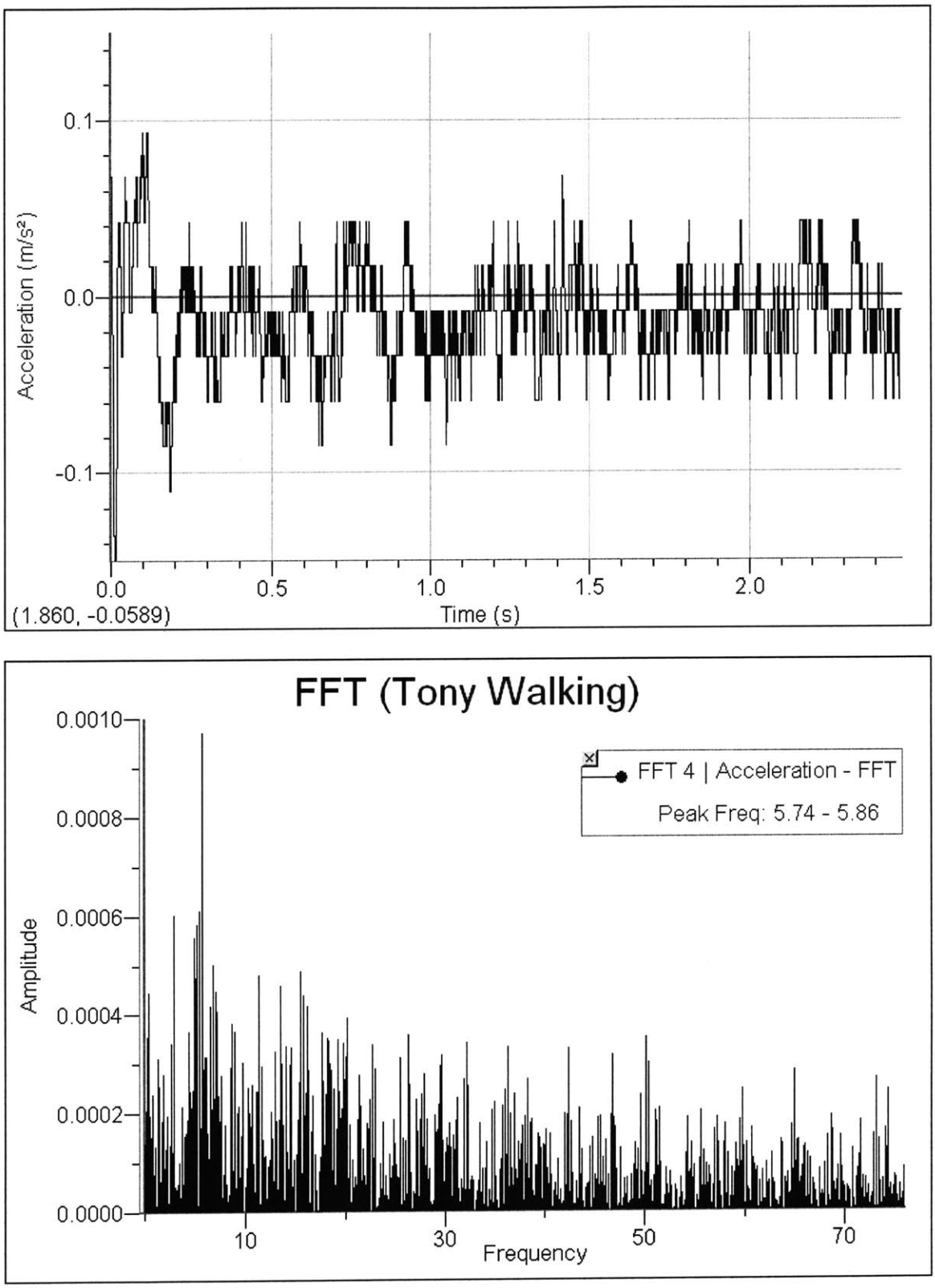

Figure 4-12: Acceleration Time-History (above) and Frequency Spectrum (below) (Tony Walking)

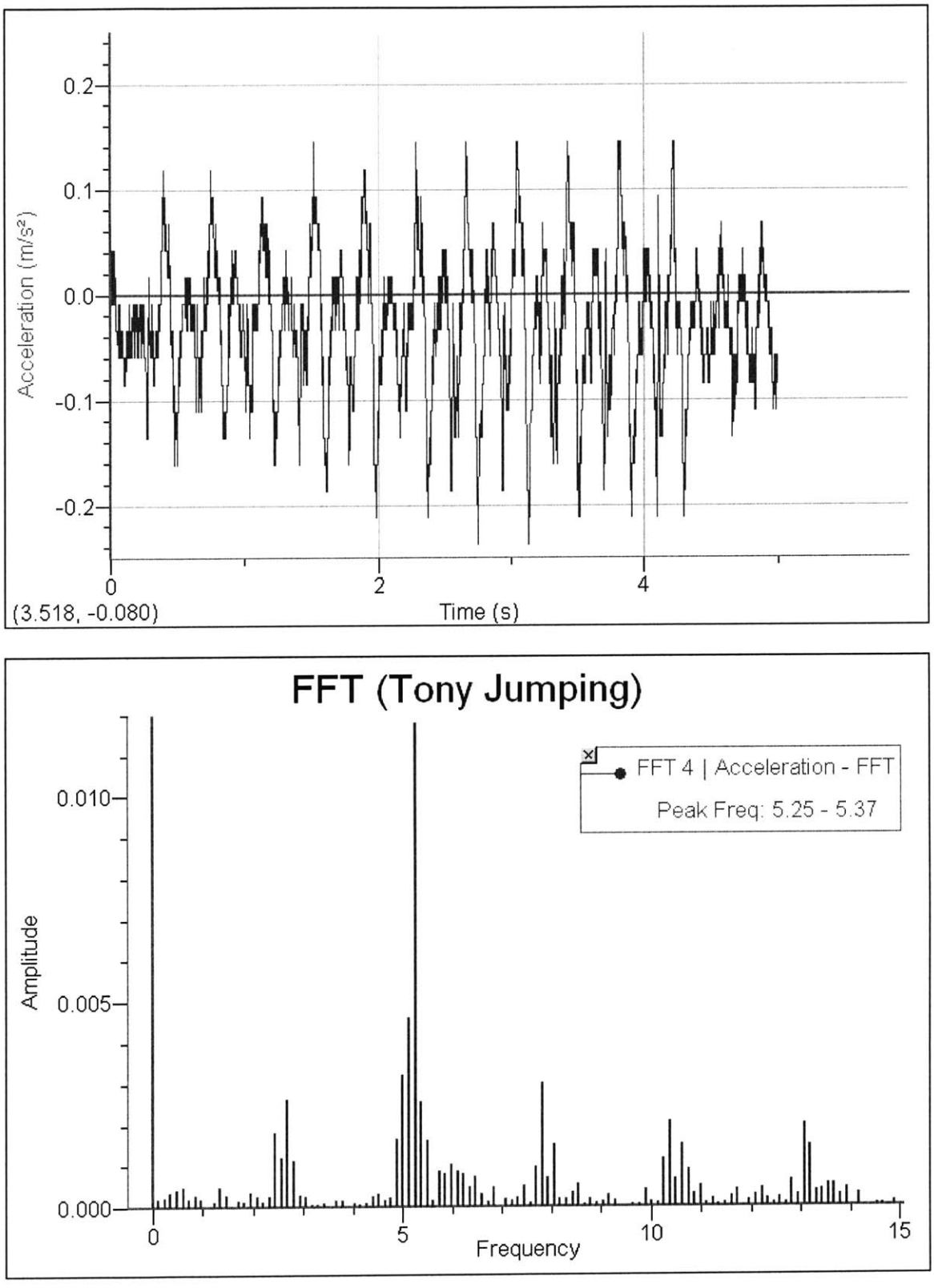

Figure 4-13: Acceleration Time-History (above) and Frequency Spectrum (below) (Tony Jumping)

After each of the previous tests was conducted, the people present (bank representative, Tony, Colin) were interviewed to determine his/her comfort level. For case 1 (Colin Walking Heavily), the two subjects collectively felt the vibration for the entire period of time that Colin was walking. The vibrations were very noticeable and would not be tolerable for a longer period of time. The subjects interviewed noted no feeling of uneasiness. For Case 2 (Tony Walking) the representative felt the vibration but sensed that it died out quickly. No absolute discomfort was felt. For Case 3 (Tony Jumping), these vibrations were the most noticeable and intolerable.

From the above figures it can be deduced that the natural frequency is approximately 5.3 Hz. for all three cases with a maximum acceleration amplitude of approximately 0.2 m/s^2 (200 mm/s^2) when excited by the bouncing loading (Tony Jumping). In Table 4-3 a comparison is made between the recently measured frequency and the frequency measured in 1988. The recent measurement is actually less than the measure frequency. This can be attributed to the addition of the large partitions, desks and file cabinets to the area. After the installation of the previously discussed retrofit, the frequency, in theory, increased such that it was not in resonance with the walking frequency, or harmonic of the walking frequency. Therefore, the vibration problem was not as bad as it was previously. When the additional mass, i.e. the partitions, desks, and file cabinets, was added, the frequency decreased as it is indirectly proportional to the mass of the system. Vibrations were even less annoying with the addition of the mass when compared to the level of vibration felt after the retrofit. Hence, it can be inferred that the percent change in frequency, relative to the original frequency before the retrofit, was greater for the added mass than it was for the retrofit.

Table 4-3: Recent versus Past Frequency Measurements

	Frequency [Hz]
Recently Measured Frequency	5.3
Previously Measured Frequency	7.1

Presented in Table 4-4 is a summary of the measured data obtained during the recent testing. The maximum acceleration experienced was approximately 2% of gravity which corresponds to a displacement of 0.18 mm (0.007 in.).

Table 4-4: Summary of Measured Data

	Present Data		
	Colin Walking	Tony Walking	Tony Jumping
Measured Frequency (Hz)	5.3000	5.3000	5.3000
Maximum Acceleration (m/s^2)	0.1200	0.0700	0.2000
Maximum Acceleration (% g)	1.2%	0.7%	2.0%
Maximum Deflection (mm)	0.1082	0.0631	0.1804
Maximum Deflection (in)	0.0043	0.0025	0.0071

The data collected was compared to the actual human response criteria and design criteria that have been presented in Section 3.1. The response criteria are based on amplitude of displacement and acceleration. Table 4-5 presents the correlation of the collected data with the displacement scales presented. The frequency and amplitude of displacement were plotted on the Modified Reiher-Meister scale. The region in which the data was plotted for each load case is indicated in the table below. The Wiss and Parmelee equation (3-1) was used to calculate a response value which corresponds to a level of perceptibility, both of which are presented below. Both of the displacement scales provided similar results for all three load cases, indicating that

under the walking and jumping loads the floor vibration is barely to distinctly perceptible. This also agrees with the actual interviews that were conducted after the loading of the floor system.

Table 4-5: Displacement Scale Comparison (Present Data)

	Present Data		
	Colin Walking	Tony Walking	Tony Jumping
Modified Reiher-Meister	Slightly Perceptible	Not Perceptible	Slightly to Distinctly Perceptible
Wiss-Parmelee	2.42 Barely/Distinctly Perceptible	2.10 Barely Perceptible	2.78 Distinctly Perceptible

When compared to the acceptable criteria discussed previously, the maximum acceleration is above the acceptable criteria suggested by most of the design aids. The following plots, Figure 4-14 through Figure 4-16, exhibit the actual response for the three load cases. Also plotted on each are the acceptable acceleration limits as suggested by the previously discussed human response criteria. The maximum amplitude of all three exceed the 0.5% gravity (0.05 m/s^2) as suggested by Murray et al. in the AISC Design Guide. The maximum amplitude for the first load case, Figure 4-14, falls between the 1% g and 1.5%g. The maximum amplitude for the second load case, Figure 4-15, is relatively small compared to the other two cases. The max acceleration falls just above the 0.5% g limit. With the third load case, Figure 4-16, the maximum amplitude of acceleration surpasses even the 1.5% g limit.

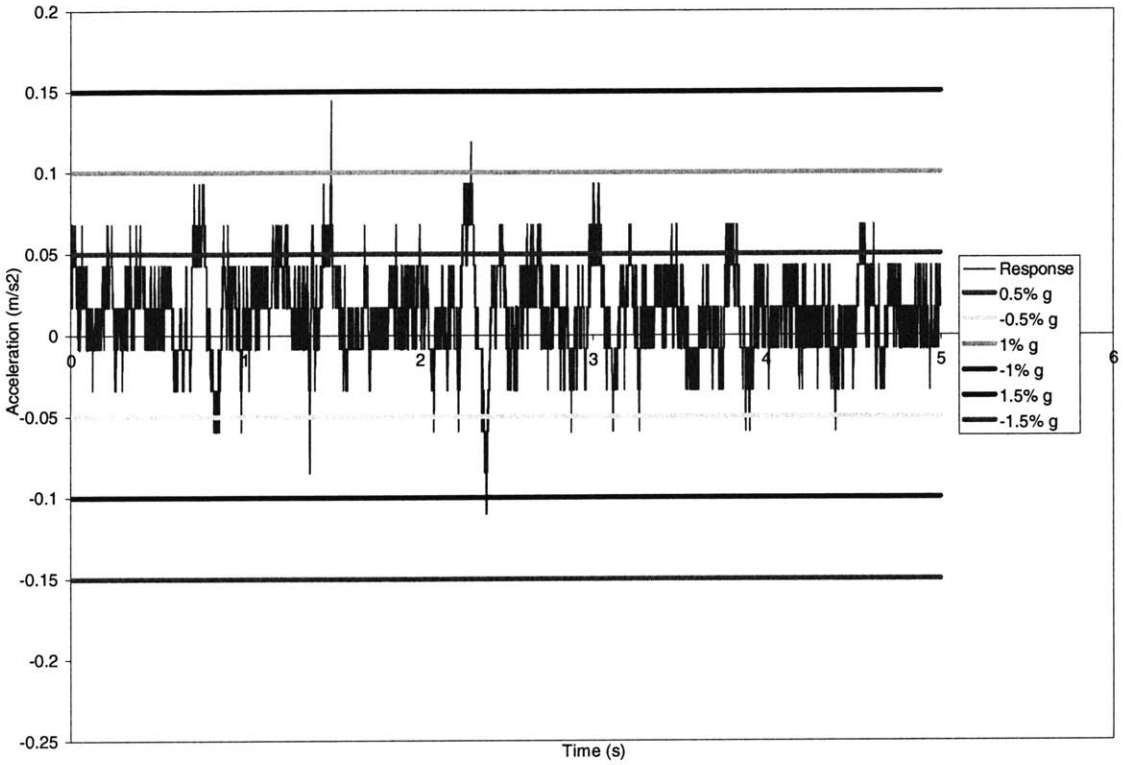

Figure 4-14: System Response with Acceptable Acceleration Criteria (Colin Walking)

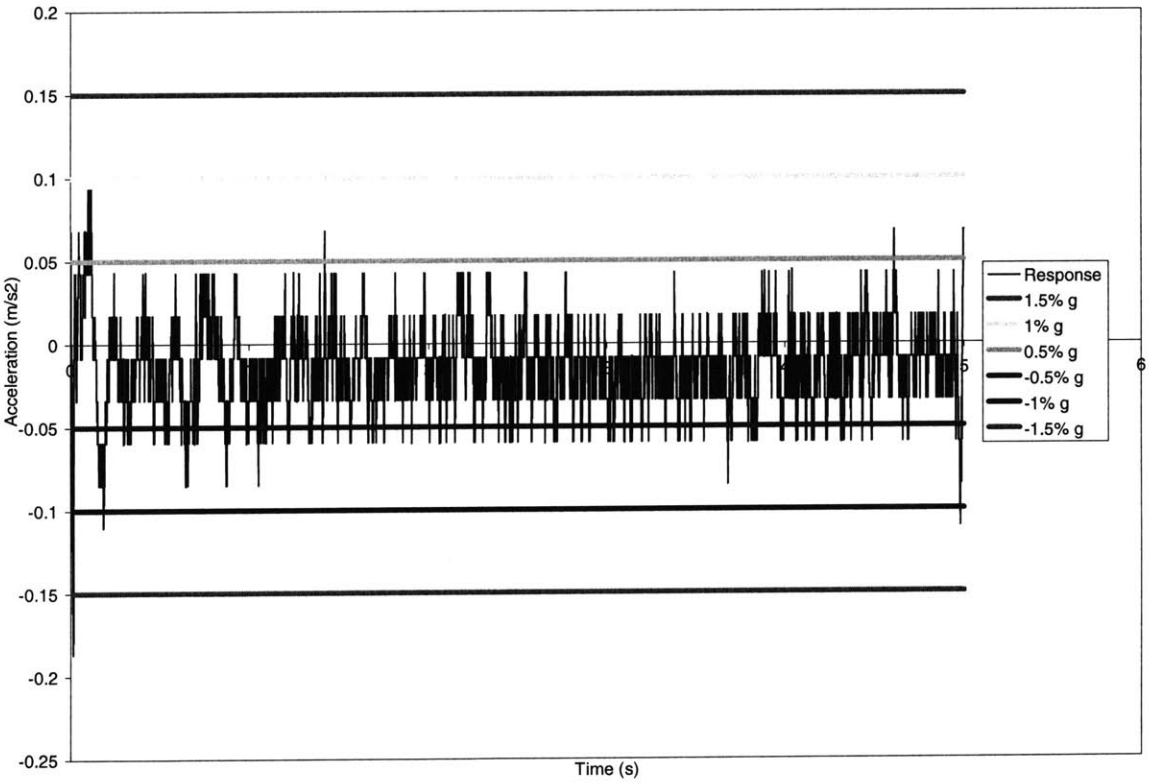

Figure 4-15: System Response with Acceptable Acceleration Criteria (Tony Walking)

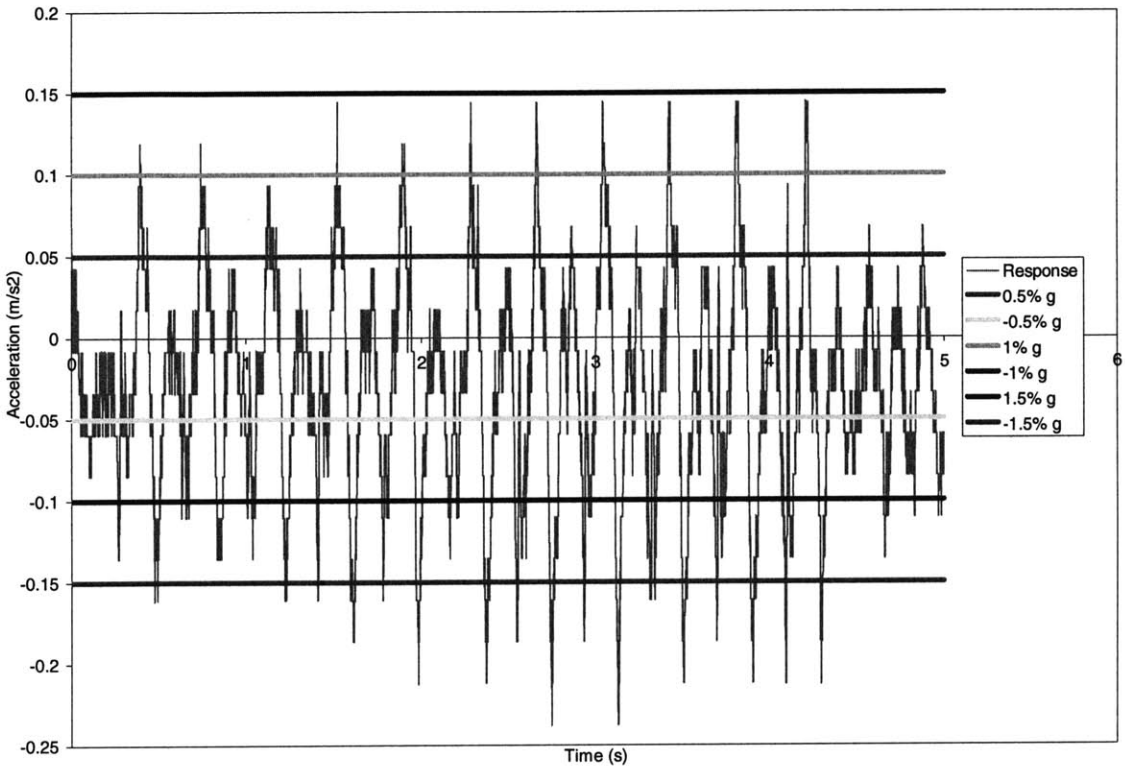

Figure 4-16: System Response with Acceptable Acceleration Criteria (Tony Jumping)

4.4.Past Data Present Data

In Table 4-5, the data that was recently collected was plotted for each of the two scales compared and the corresponding perceptibility level was then put in the table. The same process was conducted for the past data and Design Guide 11 requirements and the results can be found in Table 4-6. In order to get a better sense of the relative severity of the vibrations, all three sets of data have been included in the comparison below. Note that the assessments given for both the past and present data by both scales agree with the vibrations that were experienced at each time. The Design Guide 11 requirements were included in this table as to show where the target values actually are.

Table 4-6: Comparison of Past Data, Present Data, and Design Guide Criteria

	Present Data			*Past Data*			Design Guide 11
	Colin Walking	Tony Walking	Tony Jumping	John Walking	Tony Walking	Sheila Walking	Requirements
Modified Reiher-Meister	Slightly Perceptible	Not Perceptible	Slightly to Distinctly Perceptible	Strongly Perceptible	Distinctly to Strongly Perceptible	Distinctly Perceptible	Not Perceptible
Wiss-Parmelee	2.42 Barely/Distinctly Perceptible	2.10 Barely Perceptible	2.78 Distinctly Perceptible	4.73 Sever Vibration	3.94 Strongly Perceptible	3.65 Distinctly to Strongly Perceptible	1.92 Barely Perceptible

Notice how severe the actual vibrations were in 1988. Even for the smaller loading (Sheila walking) the vibrations were still strongly perceptible.

The relative maximum acceleration for each load case (John walking, Tony walking and Sheila walking) was 2 m/s^2, 1 m/s^2, and 0.75 m/s^2, respectively. These values are extremely high compared to the present values, hence the desperate need for a retrofit at that period of time.

4.5.Alternative Design to Control Floor Vibration

As previously mentioned there are a few alternatives that can be implemented in order to reduce the amplitude of vibration acceleration and displacement. The natural frequency of the system may be altered in such a way that it is not a harmonic multiple of the loading frequency. This can be done by altering either the mass or frequency of the system. Since this is an existing system it is difficult to simply add stiffness and/or mass. For instance, during the design phase of a project, the member size can simply be changed. Since the system is in place it is not so simple.

Assuming the maximum amplitude of acceleration to be 0.2 m/s^2 and using Figure 2-10 and equation (2-18), the stiffness of the system must be increased by factors of 1.8, 1.4, or 1.26 in order to maintain accelerations that are 0.5% g, 1% g, or 1.5% g, respectively. This is assuming that the mass is held constant, i.e. the loading to mass ratio is constant. Adding stiffness to the system may become a laborious task, i.e. welding additional material to the existing joist.

In order to reduce the acceleration of the system to a value of 0.5% g, assuming the maximum amplitude of acceleration to be 0.2 m/s^2 and using equation (2-18), the modal mass would have to be multiplied by a factor of 4. Likewise to reduce the acceleration to 1% g and 1.5% g, the modal mass would have to be multiplied by 2 and $1\frac{1}{3}$, respectively. The main concern when increasing mass is that a significant amount of dead load is added to the structural system.

Another alternative would be to add a tuned mass damper to the system. A tuned mass damper (TMD) is a device consisting of a mass, spring, and damper. The TMD is added to a structure, tuned to a certain frequency, that when excited at the specified frequency vibrates out

of phase with the structure. As the TMD is vibrating out of phase with the structure, the vibration response of the structure is reduced. As the device vibrates, energy is dissipated through the inertial force as applied to the structure.

There is a certain design procedure that must be followed when dealing with TMD systems which is similar to ones presented in Section 2.4. Firstly, the floor system is reduced to an undamped, open web steel joist, single degree of freedom system coupled with a damped tuned mass damper, as show in Figure 4-17. (Connor, 233)

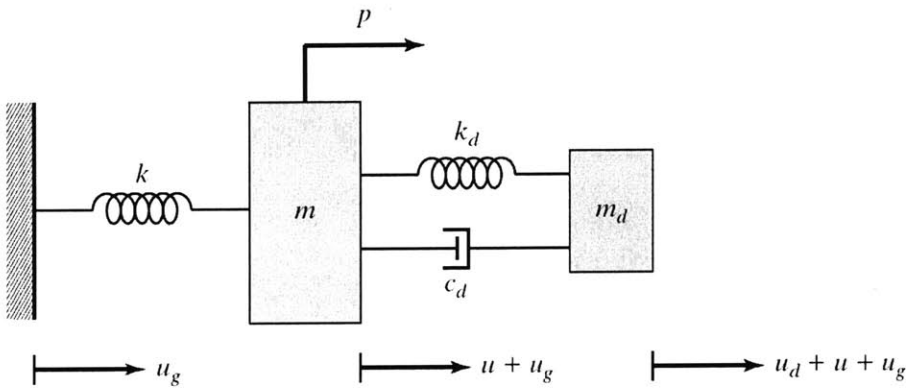

Figure 4-17: Undamped SDOF System Coupled with a Damped Tuned Mass Damper

The equations of motion for this system are as follows:

$$m_d\ddot{u}_d + c_d\dot{u}_d + k_d u_d + m_d\ddot{u} = -m_d a_g \quad \textbf{(4-1)}$$

$$m\ddot{u} + ku - c_d\dot{u}_d - k_d u_d = -ma_g + p \quad \textbf{(4-2)}$$

The dynamic response of the system is related to the following dynamic amplification factors.

$$H_1 = \frac{\sqrt{[f^2 - \rho^2]^2 + [2\xi_d \rho f]^2}}{|D_2|} \tag{4-3}$$

$$H_2 = \frac{\sqrt{[(1+\bar{m})f^2 - \rho^2]^2 + [2\xi_d \rho f(1+\bar{m})]^2}}{|D_2|} \tag{4-4}$$

$$H_3 = \frac{\rho^2}{|D_2|} \tag{4-5}$$

$$H_4 = \frac{1}{|D_2|} \tag{4-6}$$

$$|D_2| = \sqrt{([1-\rho^2][f^2-\rho^2] - \bar{m}\rho^2 f^2)^2 + (2\xi_d \rho f[1-\rho^2(1+\bar{m})])^2} \tag{4-7}$$

$$f = \frac{\omega_d}{\omega} \tag{4-8}$$

where f is the ratio of the TMD natural frequency to the system natural frequency, ξ_d is the damper damping ratio, and $\bar{m}$ is the ratio of the damper mass the to the system mass. Of primary importance for this design case is the H_1 function. This is the amplification of u from p. Since the performance constraints given are in terms of acceleration rather than displacement, this H_1 function can be used to determine a function that can be used for acceleration control. This H_1 function can be multiplied by the natural frequency of the system in order to attain the amplification of a from p, H_1'. The relationship between H_1 and H_1' can be seen in the following:

$$\hat{a} = \frac{\hat{p}}{k}\Omega^2 H_1 = \frac{\hat{p}}{m} H_1' \tag{4-9}$$

$$H_1' = \rho^2 H_1 \tag{4-10}$$

The actual shape of the H_1' function can be seen in Figure 4-18. The main goal of the TMD design is to have the values of P and Q at the same "elevation" on the plot, i.e. the H_1' value for P and Q are equal. Notice that all three of the plots of varying damper damping ratio intersect at the points P and Q. This indicates that the location of P and Q only depend on the mass ratio and frequency as shown in the amplification factor equations above. (Connor, 233-239)

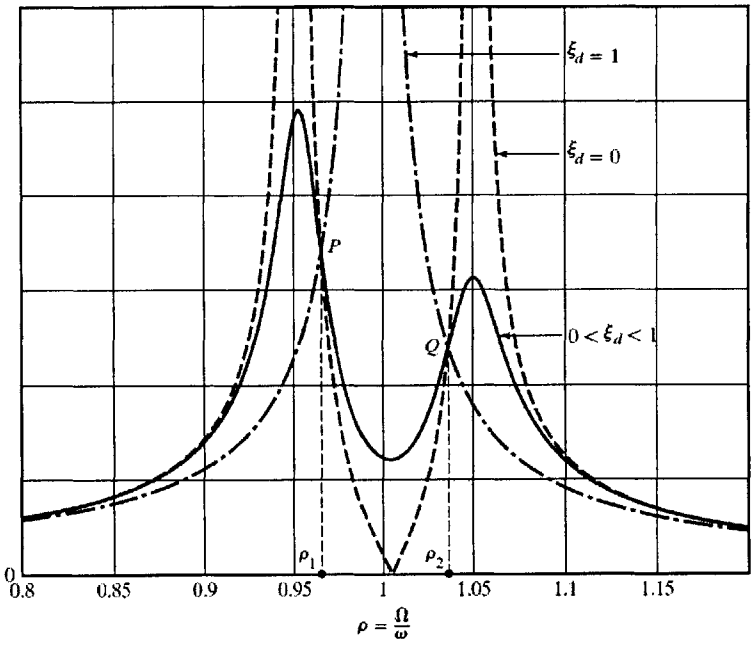

Figure 4-18: H_1' versus ρ

A series of H_1' plots were developed, all of which can be found in Appendix C, in order to determine the optimal parameters of the system for a given mass ratio. A sample plot can be seen in Figure 4-19. A MATLAB program, the actual script of which can be found in Appendix C, was used to plot approximately 20 plots of H_1' versus ρ, holding the mass ratio constant and looping through 20 different frequencies. The 20 plots were then inspected to determine the optimal frequency, which is the frequency which causes P and Q to be plotted at the same

elevation. Also determined from the optimum plot of each mass ratio, is the optimum damper damping ratio. Notice in Figure 4-19, that there are numerous plots of varying colors. The different plots indicate the varying damping ratio. The optimal damper damping ratio is the damping plot which has its two maximum points at the elevation of P and Q. This can be clearly seen in Figure 4-20 below. This process was repeated for a range of mass ratios from 0.01 to 0.1.

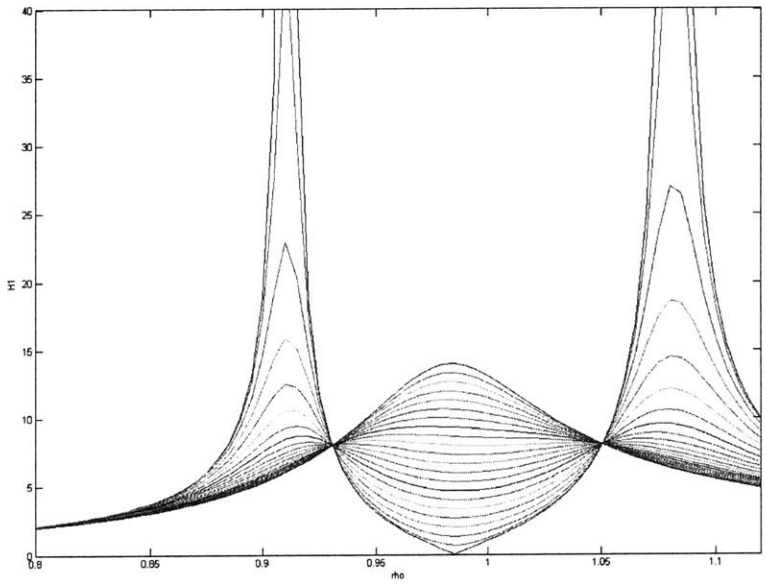

Figure 4-19: Sample Optimal Plot; Mass Ratio = 0.03, Frequency = 0.985 Hz.

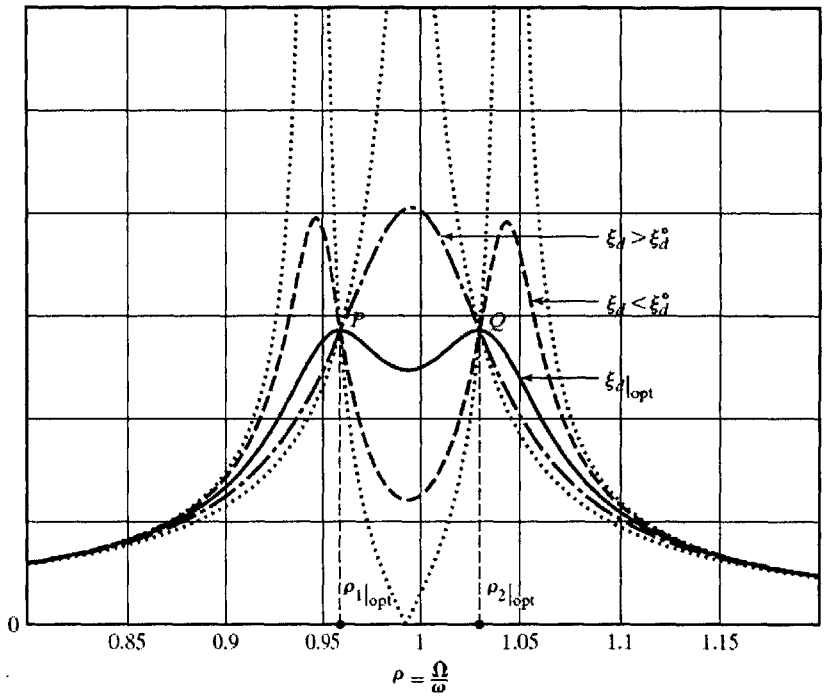

Figure 4-20: H_1' versus ρ for optimal frequency and optimal damping ratio. (Altered from Connor, 238)

With optimal values of frequency (f_{opt}), damper damping ratio (ξ_d), amplification factor (H_1'), and the relative mass ratio ($\bar{m}$), a series of design charts were then developed. The three design charts consisted of the three optimal parameters plotted against the mass ratio. The equivalent damping ratio was also determined and plotted against the mass ratio. Therefore, with the mass ratio, it can be determined approximately how much damping is being provided to the original mass. The series of plots, Figure 4-21 through Figure 4-24, can be seen below. (Connor, 233-239)

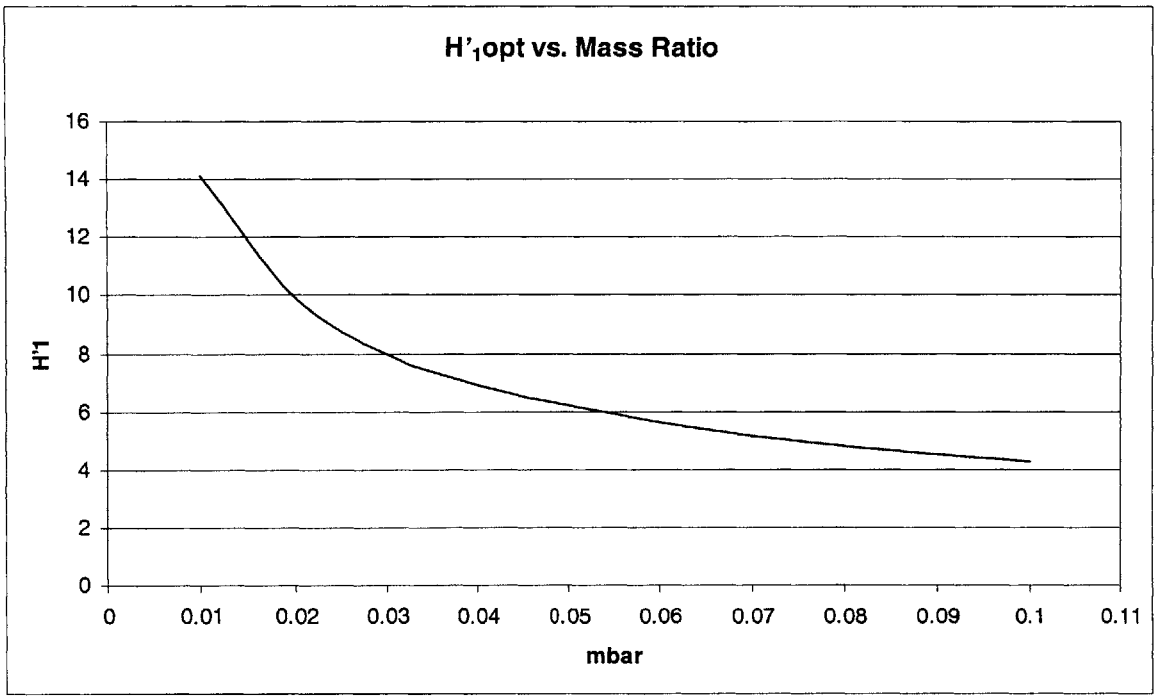

Figure 4-21 $H_1^{'}$ versus $\bar{m}$

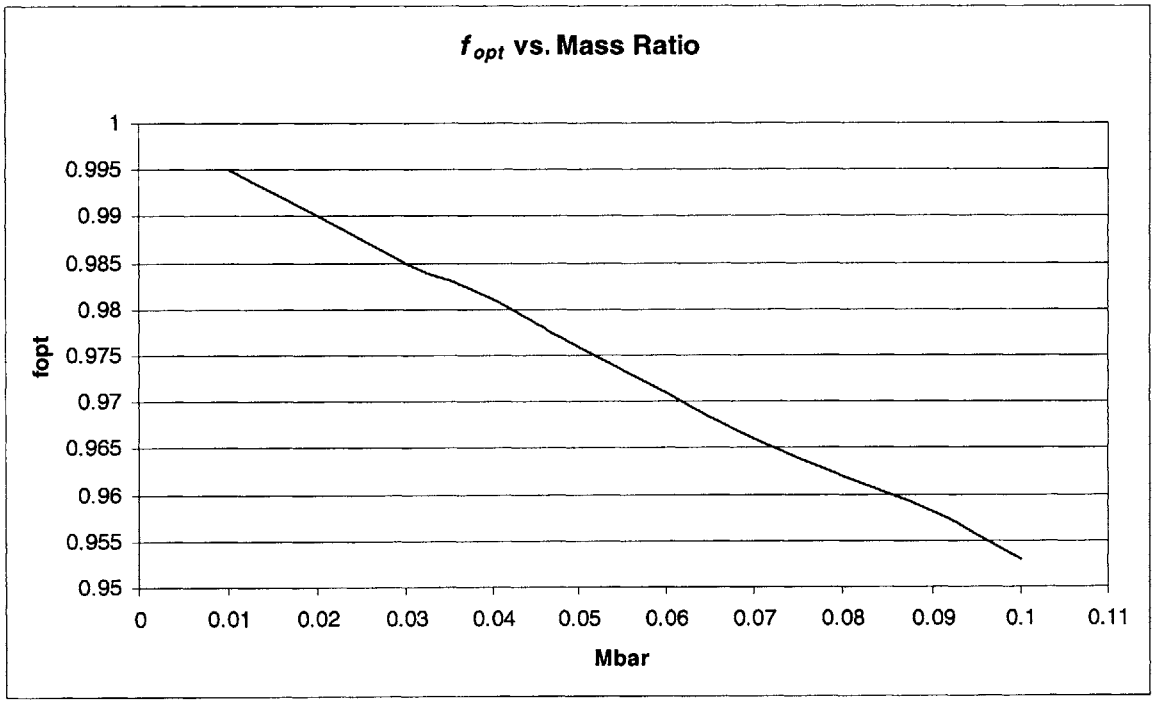

Figure 4-22: f_{opt} versus $\bar{m}$

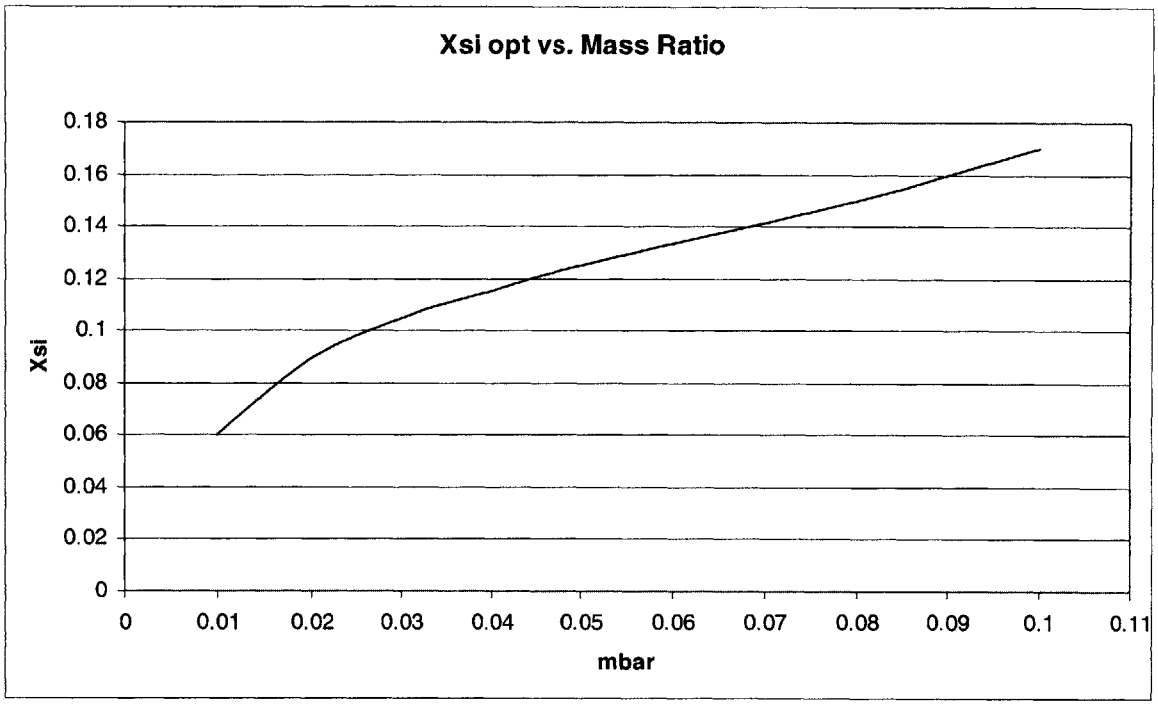

Figure 4-23 $\xi_{d\,opt}$ **versus** $\bar{m}$

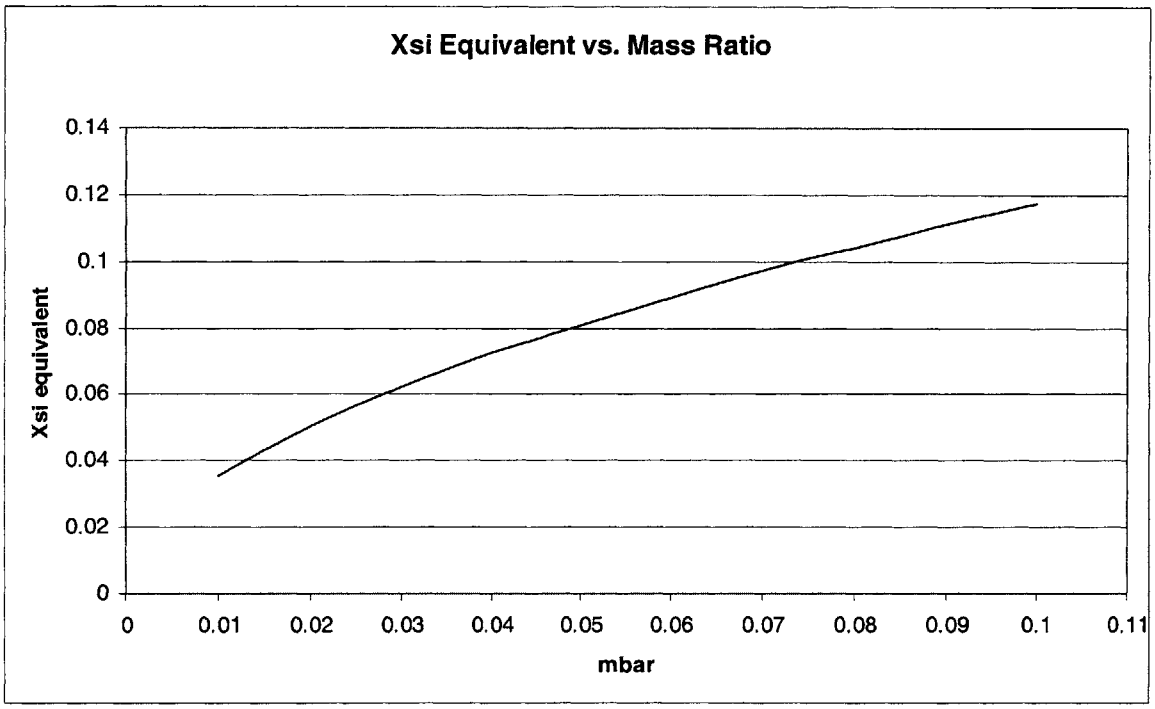

Figure 4-24: ξ_e **versus** $\bar{m}$

With a performance goal, i.e. acceleration limit, the TMD design procedure may commence. In the case of the Bank floor, the measured values of acceleration were used to determine a load to mass ratio ($\hat{p}/m$) for an assumed frequency ratio, as shown by equation (2-16). From here the load to mass ratio along with the constraining performance criteria was used in equation (4-10). A series of acceleration constraints were used to determine a series of values of H_1', with each H_1' value the optimal mass ratio for each acceleration limit was determined. With the mass ratio, the remaining optimal values can be found and for this case study, the values obtained can be found in Table 4-7 below.

Table 4-7: TMD Optimal Values for Various Acceleration (% g) Constraints

	0.5% g	1% g	1.5% g
H_{1opt}	2.5000	4.9000	7.4000
$\bar{m}$	N/A	0.0750	0.0340
f_{opt}	N/A	0.9640	0.9830
ξ_{dopt}	N/A	0.146	0.110
ξ_e	N/A	0.100	0.067

With above values, the actual TMD can be designed with the following equations (Connor, 244):

$$m_d = m\bar{m} \tag{4-11}$$

$$\omega_d = f_{opt}\omega \tag{4-12}$$

$$k_d = m_d\omega_d^{\,2} = \bar{m}kf_{opt}^{\,2} \tag{4-13}$$

$$c_d = 2\xi_{dopt}\omega_d m_d = \bar{m}f_{opt}\left[2\xi_{dopt}\omega m\right] \tag{4-14}$$

The actual design values for the 3 different acceleration constraints can be found in Table 4-8 below. The calculations conducted can be found in Appendix D. Table 4-9 describes the vibration perceptibility as per the Modified Reiher Meister scale and the Wiss and Paremelee scale. A series of these tuned mass dampers can be placed at midspan of each of the joist located at the center of the floor system. A schematic drawing, not to scale, is shown in Figure 4-25. Notice how for the 0.5% g acceleration limit that the TMD could not be designed. This is simply because this criteria is simply too low to be attained with the installation of such a device. In general, as it has been explained previously, in order to meet this very low criterion, major expensive and laborious structural changes would have to take place. The vibration of the floor structure can be brought down to 1.5% g with a reasonable fix. Installing the TMD will provide this acceleration along with 6% effective damping to the system. This complies with the standard set forth in Figure 3-3: Canadian Standards Association Scale developed by Allen and Rainer (Murray et. al, 69) which allows for accelerations in the order of 1.5% g with damping at 3% of critical.

Table 4-8: TMD Design Values

	0.5% g	1% g	1.5% g
m_d (kg)	N/A	48.75	22.10
ω_d (rad/s)	N/A	32.10	32.73
k_d (kN/m)	N/A	50.24	23.68
c_d (N-s/m)	N/A	456.97	159.16

Table 4-9: System Vibration Perceptibly with TMD Installed

	TMD Installation	
	1% g	1.5% g
Modified Reiher-Meister	Not Perceptible	Slightly Perceptible
Wiss-Parmelee	2.31 Barely Perceptible	2.57 Barely/Distinctly Perceptible

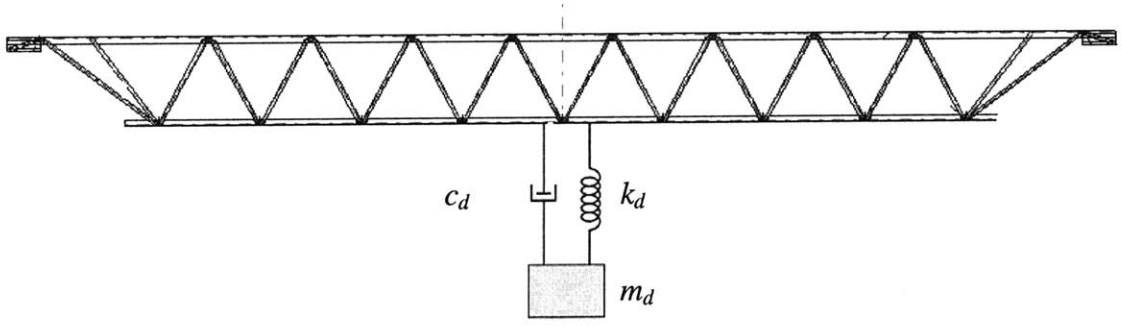

Figure 4-25: Schematic of Single Joist with TMD attached, NTS (Portions from Connor, 233)

4.6. Conclusions and Recommendations

In order to control the floor vibration of the existing Bank, it is suggested that a series of tuned mass dampers be installed. The installation of a series of 22.10 kg masses, with a frequency of 5.2 Hz, and 159 N-s/m dampers will reduce the acceleration to approximately 1.5 % g. Should the acceleration want to be reduced to 1% g, a larger mass-spring-damper system may be installed, the properties of which are included in Table 4-8 above. However, the vibrations at or below 1.5% g were noted to be slightly perceptible. Hence, it is recommend to install the TMD which reduces the system acceleration to 1.5% g.

5. Conclusions

A case study was presented to compare the results of testing with design criteria that exist. The experimental data was compared to the human response criteria based on motion measures and the perceptibility of the vibrations was accurately described. The data was then compared to the currently available AISC Design Guide as it was determined that the existing vibrations occurring under normal foot traffic actually exceed the design acceleration criteria. When designing a retrofit solution it was determined that the criteria set forth by the Design Guide, accelerations not to exceed 0.5% g, could not be met with reasonable adjustments to the structure. It was then determined that 1% g or 1.5% g accelerations could be achieved with the installation of a series of tuned mass dampers. The 1% g or 1.5% g do meet criteria set forth by the Canadian Standards Association. Ultimately, the vibration issue is a serviceability issue; hence, the primary judges of the comfort level or acceptability of the vibrations are the sensors, i.e. the people that they affect.

As a result of this case study it has been determined that the Alan and Rainer scale, along with the Modified Reiher Meister scale and the Wiss and Paremelee scale, accurately describe the human response criteria. Also determined was that the American Institute of Steel Construction Floor Vibrations Due to Human Activity (Design Guide 11) has extremely conservative acceleration criteria that basically aim to make the vibration not noticeable at all. When designing new structures, this guide is easier to adhere to as it would require changing configurations and or member sizes to increase the stiffness of the system. With a retrofit scenario, this guide is rather difficult to abide by with respect to both construction and design.

6. References

Bachmann, Hugo, and Walter Ammann. Vibrations in Structures Induced by Man and Machines. Structural Engineering Documents. 3rd Edition. Zurich, International Association for Bridge and Structural Engineering.

Chopra, Anil K. Dynamics of Structures: Theory and Applications to Earthquake Engineering. 2nd Edition. Upper Saddle River: Prentice Hall, 2001.

Connor, Jerome J. Introduction to Structural Motion Control. Upper Saddle River: Pearson Education, 2003.

Ebrahimpour, Ayra, and Ronald L. Sack. "A review of vibration serviceability criteria for floor structures." Computers and Structures 83. Elsevier, 2005. 2488-2494.

Ellingwood, Bruce, and Andrew Tallin. "Structural Serviceability: Floor Vibrations." Journal of Structural Engineering. Vol. 110. No. 2. American Society of Civil Engineers, 1984. 401-419.

Galambos, Theodore V. "Vibration of Steel Joist Concrete Slab Floors." Steel Joist Institute Technical Digest No. 5. Myrtle Beach: Steel Joist Institute.

Hanagan, Linda M. "Floor Vibration Serviceability: Tips and Tools for Negotiating a Successful Design." 2003 NASCC Proceedings. Session D6. Baltimore, April.

Hanagan, Linda M, Christopher Raebel, and Martin Tretheway. "Dynamic Measurements of In-Place Steel Floors to Assess Vibration Performance." Journal of Performance of Constructed Facilities. Vol. 17. No. 3. American Society of Civil Engineers, Aug. 1, 2003. 126-135.

Hanagan, Linda M. "Walking Induced Floor Vibration Case Studies." Journal of Architectural Engineering. Vol. 11. No. 1. American Society of Civil Engineers, March, 2005. 14-18.

Murray, Thomas M. "Acceptability Criterion for Occupant-Induced Floor Vibrations." Sound and Vibration. Nov., 1979. Engineering Journal. American Institute of Steel Construction, 2003. 62-70. AISC Online Library. 62-70.

Murray, Thomas M. "Design to Prevent Floor Vibrations." Engineering Journal. American Institute of Steel Construction, 2003. 82-87. AISC Online Library.82-87.

Murray, Thomas M., David E. Allen, Eric E. Ungar. Smith, J.W. Dynamic Loading and Design of Structures. Ed. A.J. Kappos. London: Spon Press, 2002. 285-322.

7. Appendix A: List of Acceptance Criteria (Murray et al.)

Date	Reference	Loading	Application	Comments
1931	Reiher and Meister	Steady State	General	Human response criteria
1966	Lenzen	Heel-drop	Office	Design criterion using Modified Reiher and Meister scale
1970	HUD	Heel-drop	Office	Design criterion for manufactured housing
1974	International Standards Organization	Various	Various	Human response criteria
1974	Wiss and Parmelee	Footstep	Office	Human response criteria
1974	McCormick	Heel-drop	Office	Design criterion using Modified Reiher and Meister scale
1975	Murray	Heel-drop	Office	Design criterion using Modified Reiher and Meister scale
1976	Allen and Rainer	Heel-drop	Office	Design criterion using modified ISO scale
1981	Murray	Heel-drop	Office	Design criterion based on experience
1984	Ellingwood and Tallin	Walking	Commercial	Design criterion
1985	Allen, Rainer and Pernica	Crowds	Auditorium	Design criterion related to ISO scale
1986	Ellingwood et al	Walking	Commercial	Design criterion
1988	Ohlsson	Walking	Residential/Office	Lightweight Floors
1989	International Standard ISO 2231-2	Various	Buildings	Human response criteria
1989	Clifton	Heel-drop	Office	Design criterion
1989	Wyatt	Walking	Office/Residential	Design criterion based on ISO 2631-2
1990	Allen	Rhythmic	Gymnasium	Design criterion for aerobics
1993	Allen and Murray	Walking	Office/Commercial	Design criterion using ISO 2631-2

8. Appendix B: Structural Calculations

Determination of Composite Floor System Natural Frequency

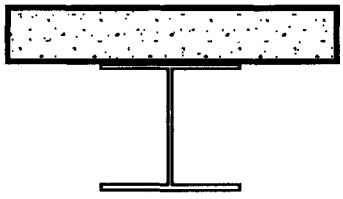

Composite Action

Material Properites

Material Properites

$Es := 300000006.8951000\ pa$ $Ec := 30000006.8951000\ pa$

$\rho s := 0.28 \cdot 12^3 \cdot 16.01846\ kgm^3$ $\rho c := 150 \cdot 16.01846\ kgm^3$

Modular Ratio $n := \frac{Es}{Ec}$ $n = 10$

Steel Joist Properties

$Is := 1100.0254^4\ m^4$

$As := 2.2 \cdot .0254^2\ m^2$

$Ys := \frac{9}{39.4}\ m$

$L := \frac{25.5}{3.28}\ m$

Concrete Slab Properties

$tc := \frac{3.25}{39.4}\ m$ $wc := \frac{30}{39.4}\ m$

$Ac := tc \cdot wc$

$Yc := \frac{19.5}{39.4}\ m$

$Ic := \frac{1}{12} \cdot wc \cdot tc^3$ $Ic = 3.561 \times 10^{-5}$

Combined Section Properties

$$Y_{bar} := \frac{Ec \cdot Ac \cdot Yc + Es \cdot As \cdot Ys}{Ec \cdot Ac + Es \cdot As} \qquad Y_{bar} = 0.446$$

$$I_{comp} := \frac{1}{12} \cdot \frac{wc}{n} \cdot tc^3 + \frac{Ac}{n} \cdot (Y_{bar} - Yc)^2 + Is + As \cdot (Y_{bar} - Ys)^2 \qquad I_{comp} = 1.316 \times 10^{-4}$$

Flexural Stiffness Perpendicular to joists (Slab Only), Dx

$$Dx := \frac{Ec \cdot tc^3}{12} \qquad Dx = 9.675 \times 10^5$$

Flexural Stiffness Parallel to the Joists (Composite Sections), Dy

$$Dy := Ec \cdot Ic + Ec \cdot Ac \cdot (Y_{bar} - Yc)^2 + Es \cdot Is + Es \cdot As\ (Y_{bar} - Ys)^2 \qquad Dy = 2.722 \times 10^7$$

$$\varepsilon := \left(\frac{Dx \cdot wc}{Dy} \right)^{\frac{1}{4}} \qquad \varepsilon = 0.406$$

Distance from the center joist to the edge of the effective floor, xo

$$xo := \frac{3 \cdot \sqrt{2} \cdot \varepsilon \cdot L}{4} \qquad xo = 3.345\ m$$

Effective number of joists, N

$x_1 := wc \qquad x_2 := 2 \cdot wc \qquad x_3 := 3 \cdot wc \qquad x_4 := 4 \cdot wc$

$wc = 0.761$

$x_4 = 3.046$

$$N := 1 + 2\cdot\cos\left(\frac{\pi\cdot x_1}{2\cdot xo}\right) + 2\cdot\cos\left(\frac{\pi\cdot x_2}{2\cdot xo}\right) + 2\cdot\cos\left(\frac{\pi\cdot x_3}{2\cdot xo}\right) + 2\cdot\cos\left(\frac{\pi\cdot x_4}{2\cdot xo}\right)$$

$N = 5.619$ Joists Effective

Say $N := 6$

Weight Supprted by joists, Dead Load

$w := (\rho s\cdot As + \rho c\cdot Ac)$ $\qquad w = 161.913 \quad \frac{kg}{m}$

Frequency of Composite Joist, fn

$$fn := \frac{\pi}{2\cdot L^2}\cdot\sqrt{\frac{Dy}{w}} \qquad fn = 10.655$$

$$\omega n_{comp} := 2\cdot\pi\cdot fn$$

But Measured Natural Frequency prior to retrofit was 7.1 Hz

Determine Non-Composite Natural Frequency

Natural Frequency for Continous Beam

$$k_{joist} := \left[Es\cdot Is\cdot\left(\frac{\pi}{L}\right)^4\cdot\frac{L}{2}\right]$$

$k_{joist} = 9.816\times 10^5 \quad \frac{N}{m}$

$$M_{modal} := \frac{w}{2}\cdot L \qquad M_{modal} = 629.386$$

$$\omega n_{joist} := \sqrt{\frac{k_{joist}}{M_{modal}}}$$

$\omega n_{joist} = 39.493$

$$fn_{joist} := \frac{\omega n_{joist}}{2\pi} \qquad fn_{joist} = 6.285$$

Hence Joist floor system is not acting completely composite. This can also be observed in the structure as there were spaces between the joist and metal deck. The fact that the natural frequency was presently measure to be 5-6Hz can be attributed to the mass added by installing the paritions and furniture.

Determine p/W ratio:

Since Open Web Steel Joist

$a := .2 \quad \frac{m}{s^2} \quad \frac{a}{9.81} = 0.02 \quad \xi := 0.01$

$\Omega := 6 \cdot 2\pi$ Measured Natural Frequency

$\rho := \frac{\Omega}{\omega n_{joist}}$,

$H_2 := \sqrt{\frac{\rho^4}{\left(1-\rho^2\right)^2 + (2\xi\cdot\rho)^2}} \qquad H_2 = 10.035 \qquad \rho = 0.955$

$PM_{actual} := \frac{a}{H_2}$

$PM_{actual} = 0.02 \qquad \frac{1}{PM_{actual}} = 50.175$

Stiffness Addition

$a_{criteria} := \begin{pmatrix} 0.05 \\ 0.1 \\ 0.15 \end{pmatrix} \frac{m}{s^2} \qquad H_2 := \frac{a_{criteria}}{PM_{actual}} \qquad H_2 = \begin{pmatrix} 2.509 \\ 5.018 \\ 7.526 \end{pmatrix}$

$\rho_{needed} := \sqrt{\frac{1 + 2\cdot\xi^2 + \sqrt{\left(1-2\cdot\xi^2\right)^2 - 1 + \frac{1}{H_2^2}}}{1 - \frac{1}{H_2^2}}} \qquad \rho_{needed2} := \sqrt{\frac{\left(1 + 2\cdot\xi^2\right) - \sqrt{\left(1-2\cdot\xi^2\right)^2 - 1 + \frac{1}{H_2^2}}}{1 - \frac{1}{H_2^2}}}$

$$\rho_{needed} = \begin{pmatrix} 1.289 \\ 1.117 \\ 1.073 \end{pmatrix} \qquad \rho_{needed2} = \begin{pmatrix} 0.846 \\ 0.914 \\ 0.94 \end{pmatrix}$$

$$\frac{\rho_{needed} - \rho}{\rho} = \begin{pmatrix} 0.351 \\ 0.17 \\ 0.124 \end{pmatrix}$$

Percent by which the frequency has to increase.

$$\left[\left(\frac{\rho_{needed} - \rho}{\rho}\right) + 1\right]^2 = \begin{pmatrix} 1.824 \\ 1.37 \\ 1.264 \end{pmatrix}$$

Amount by which the stiffness has to increase, assuming mass held constant. Using reationship $\omega =$ (k/m)^0.5

Mass Addition

Since Open Web Steel Joist

$$a_{criteria} := \begin{pmatrix} 0.05 \\ 0.1 \\ 0.15 \end{pmatrix} \frac{m}{s^2} \qquad \xi := 0.01$$

$$H_2 := \sqrt{\frac{\rho^4}{\left(1 - \rho^2\right)^2 + (2\xi \cdot \rho)^2}}$$

$H_2 = 10.035$

$\rho = 0.955$

$$PM_{ratio} := \frac{a_{criteria}}{H_2}$$

$$PM_{ratio} = \begin{pmatrix} 4.983 \times 10^{-3} \\ 9.965 \times 10^{-3} \\ 0.015 \end{pmatrix}$$

$$\frac{1}{PM_{ratio}} = \begin{pmatrix} 200.701 \\ 100.35 \\ 66.9 \end{pmatrix}$$

$$\frac{PM_{actual}}{PM_{ratio}} = \begin{pmatrix} 4 \\ 2 \\ 1.333 \end{pmatrix}$$

Corresponds to amount by which the mass has to be multiplied in order to achieve secified acceleration control.

$$\frac{a}{a_{criteria}} = \begin{pmatrix} 4 \\ 2 \\ 1.333 \end{pmatrix}$$

9. Appendix C: Development of Tuned Mass Damper Design Charts

m	f	H1	Xsi opt	Xsi equi
0.01	0.995	14.1	0.06	0.035461
0.02	0.99	9.9	0.09	0.050505
0.03	0.985	8	0.1046	0.0625
0.04	0.981	6.9	0.115	0.072464
0.05	0.976	6.2	0.125	0.080645
0.06	0.971	5.6	0.1337	0.089286
0.07	0.966	5.15	0.1416	0.097087
0.08	0.962	4.8	0.15	0.104167
0.09	0.958	4.5	0.16	0.111111
0.1	0.953	4.26	0.17	0.117371

The plots that follow are printed in order of the table above. The table includes the optimal values retrieved from the plots that follow. Also included is the Matlab language.

Matlab Program used to develop charts

```
clear
delrho=0.005;
mbar=0.01;  %Input Mass Ratio
delxi=0.01; %Incremental Damping Ratio
nf=22;      %Input Number of Damping Values
delff=0.001; %Incremental Frequency
for i=1:20
    ff1=0.99; %Input Initial Frequency
    ff(i)=ff1+(i-1)*delff;
    ff=ff(i)
    for j=1:66
        rho(1)=0.80;
        rho(j)=rho(1)+(j-1)*delrho;
        r=rho(j);
        a1=(ff^2)-r^2;
        a2=2*r*ff;
        a3=(ff^2-r^2)*(1-r^2)-mbar*(r^2)*(ff^2);
        a4=(2*r*ff)*(1-(r^2)*(1+mbar));
        for k=1:nf
            xi(1)=0.0;    %Initial Damping Ratio
            xi(k)=xi(1)+(k-1)*delxi;
            a5=a1^2+(a2*xi(k))^2;
            a6=a3^2+(a4*xi(k))^2;
            H1(j,k)=(sqrt(a5/a6))*r^2;
        end
    end
    figure(i)
    grid on
    plot(rho,H1)
    xlabel('rho')
    ylabel('H1')
    axis([0.80,1.12,0,40])

end
```

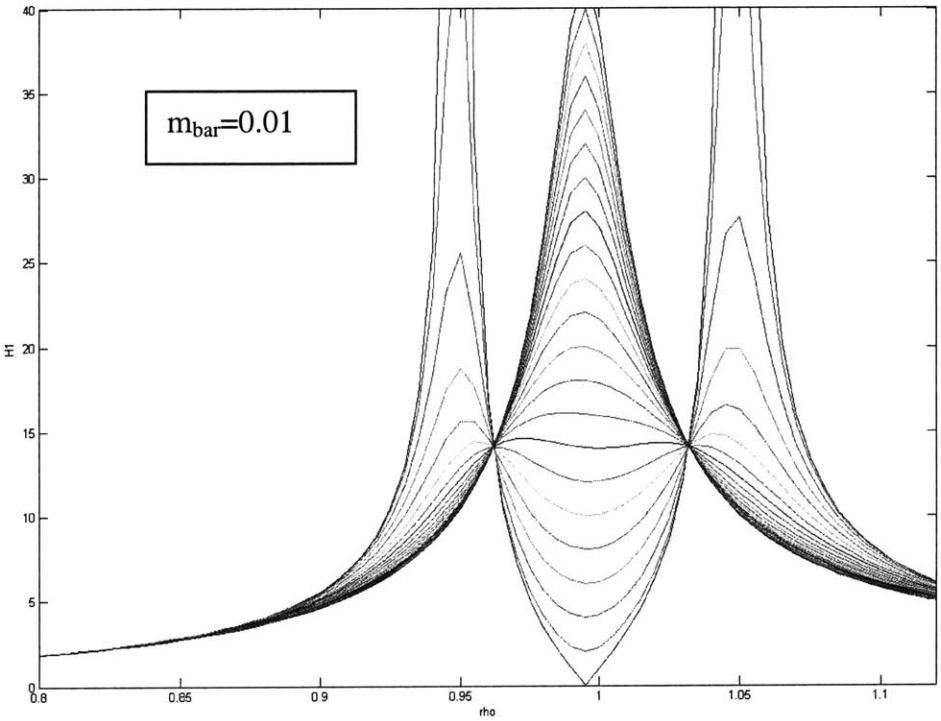
m_{bar}=0.01
H1
rho
0
5
10
15
20
25
30
35
40
0.8
0.85
0.9
0.95
1
1.05
1.1

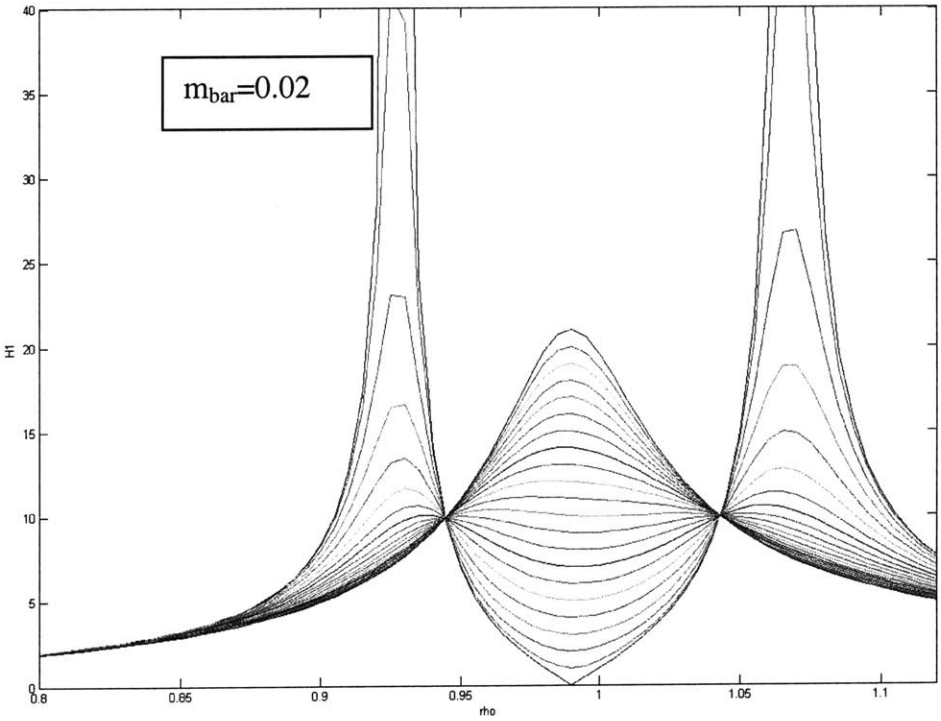
m_{bar}=0.02
H1
rho
0
5
10
15
20
25
30
35
40
0.8
0.85
0.9
0.95
1
1.05
1.1

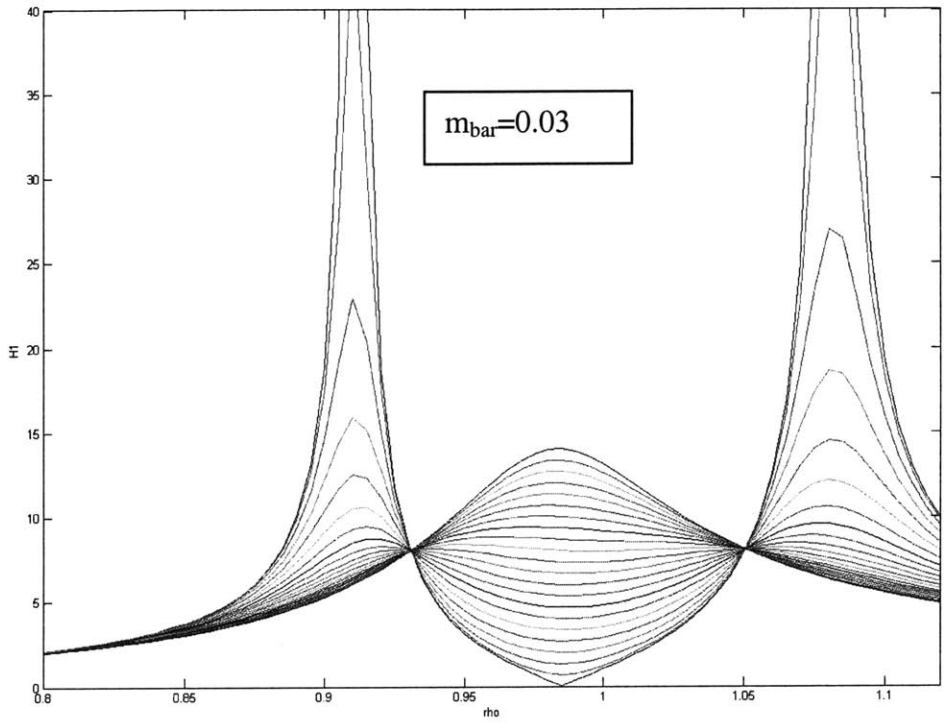
m_{bar}=0.03
H1
rho
0
5
10
15
20
25
30
35
40
0.8
0.85
0.9
0.95
1
1.05
1.1

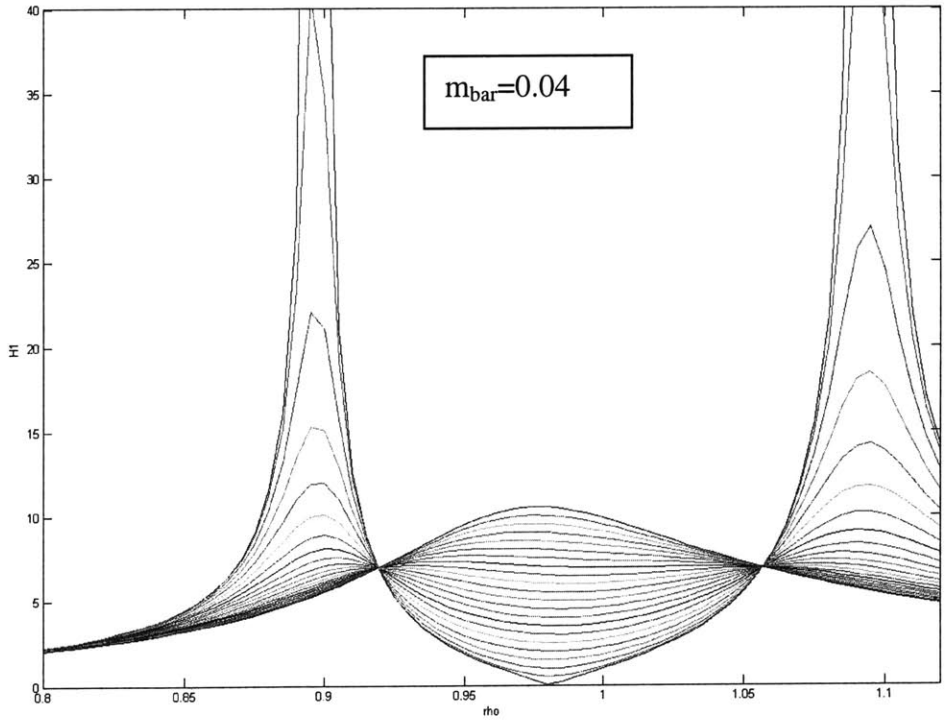
m_{bar}=0.04
H1
rho
0
5
10
15
20
25
30
35
40
0.8
0.85
0.9
0.95
1
1.05
1.1

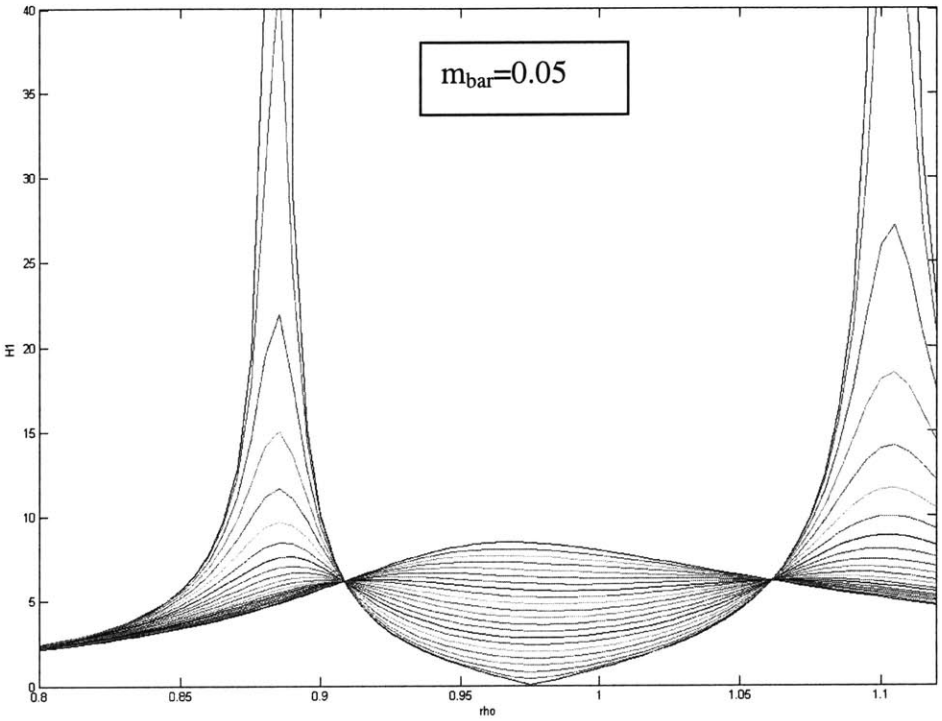
m_{bar}=0.05
H1
rho
0
5
10
15
20
25
30
35
40
0.8
0.85
0.9
0.95
1
1.05
1.1

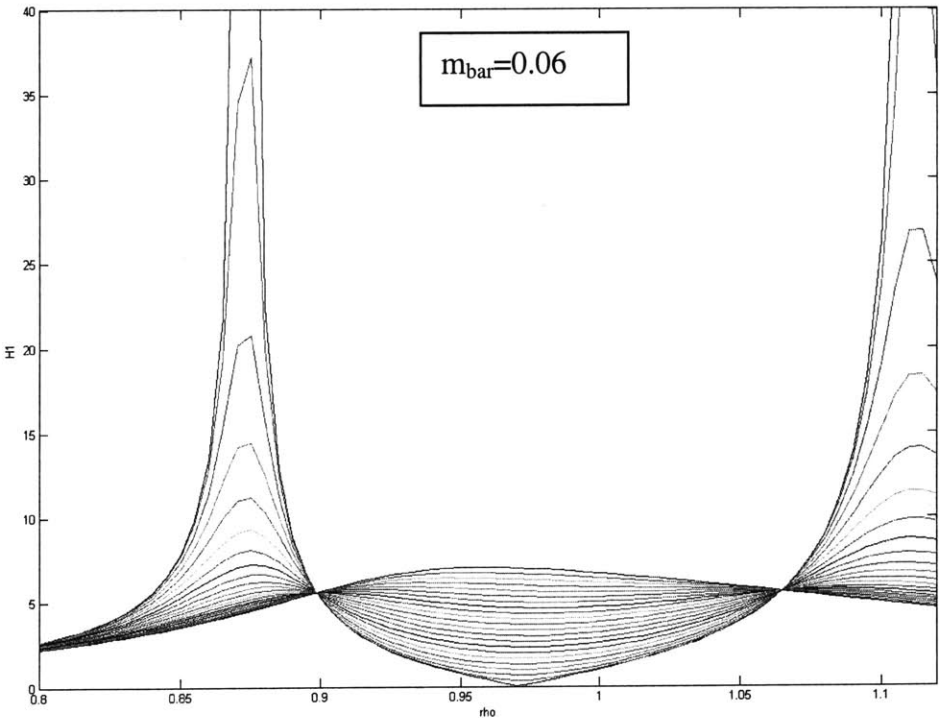
m_{bar}=0.06
H1
rho
0
5
10
15
20
25
30
35
40
0.8
0.85
0.9
0.95
1
1.05
1.1

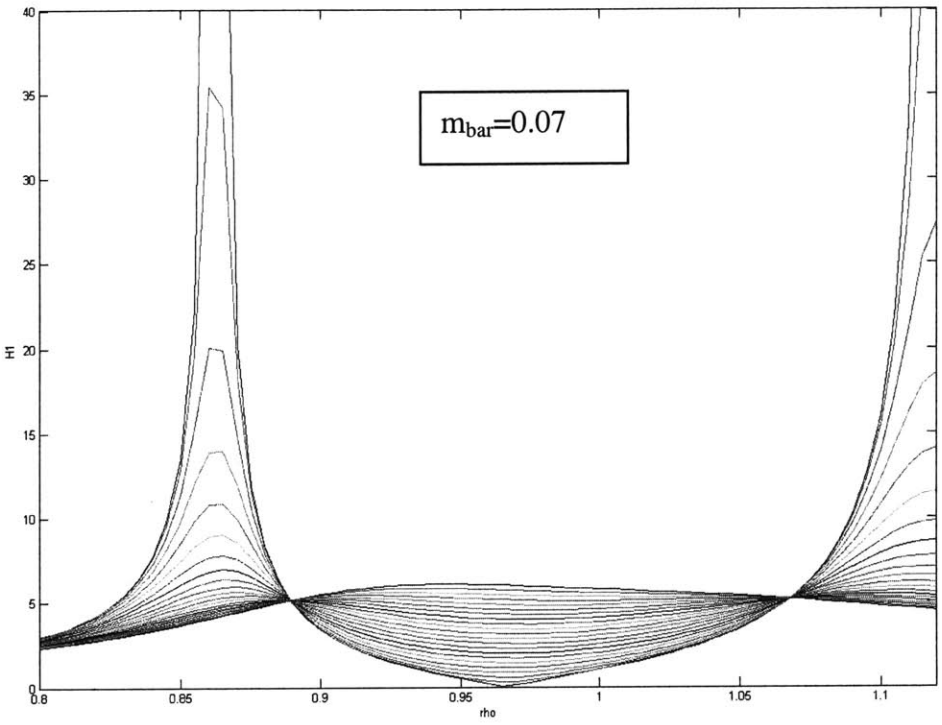
m_{bar}=0.07
H1
rho
0
5
10
15
20
25
30
35
40
0.8
0.85
0.9
0.95
1
1.05
1.1

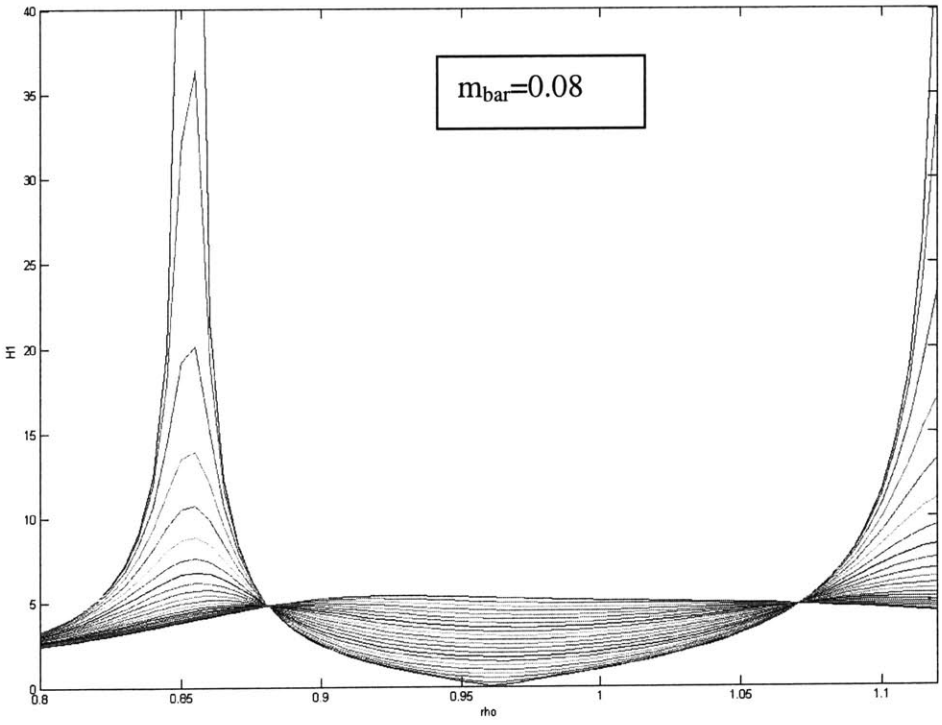
m_{bar}=0.08
H1
rho
0
5
10
15
20
25
30
35
40
0.8
0.85
0.9
0.95
1
1.05
1.1

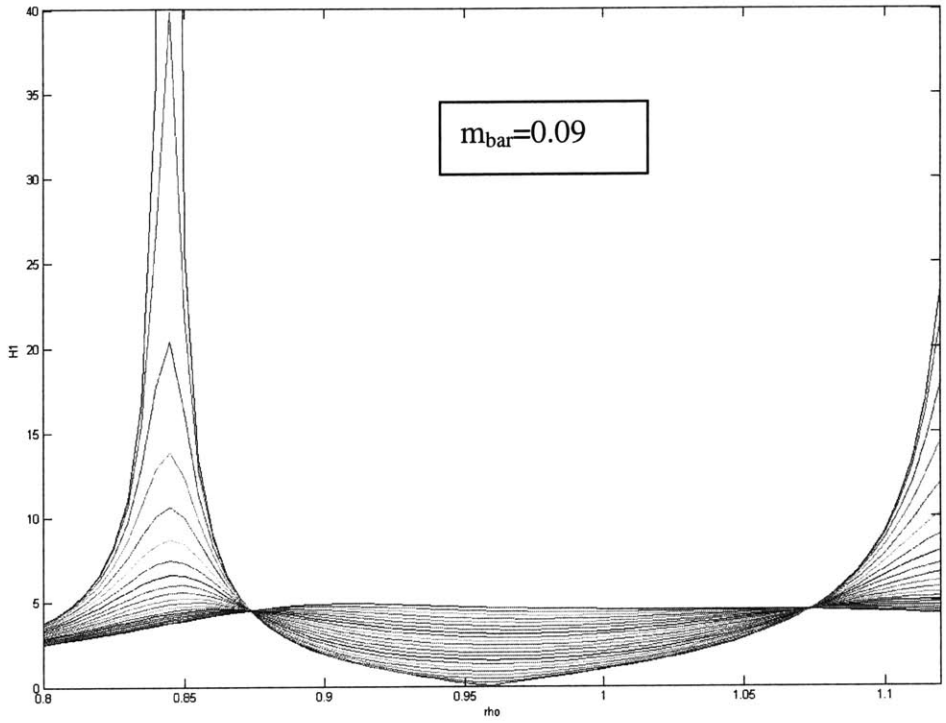
m_{bar}=0.09
H1
rho
0
5
10
15
20
25
30
35
40
0.8
0.85
0.9
0.95
1
1.05
1.1

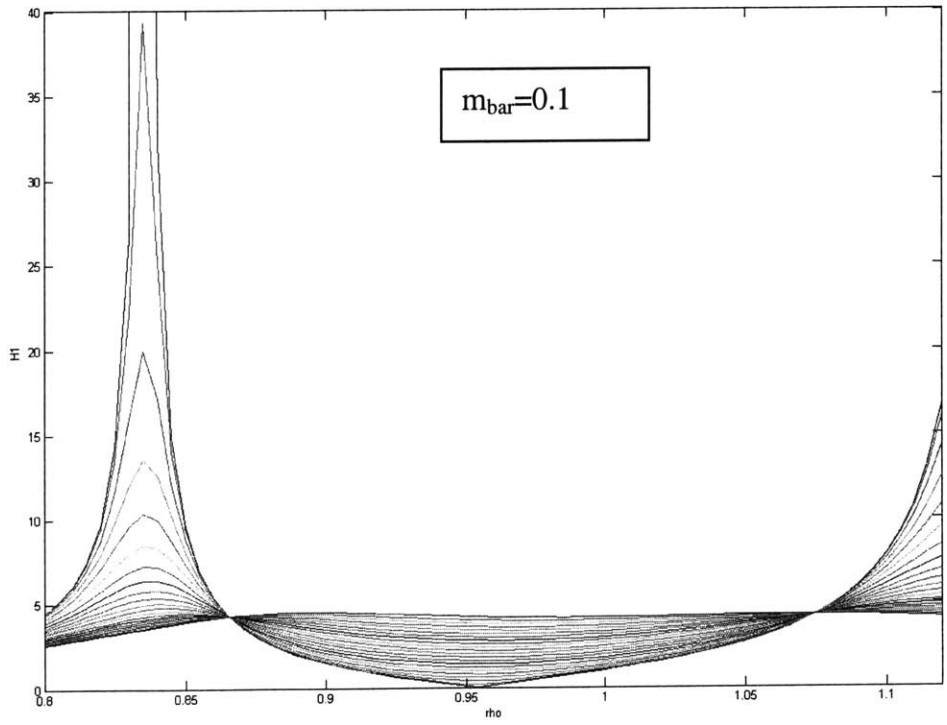
m_{bar}=0.1
H1
rho
0
5
10
15
20
25
30
35
40
0.8
0.85
0.9
0.95
1
1.05
1.1

Hand Calculations

1

$$H_1 = \frac{\sqrt{[f^2-\rho^2]^2 + [2\xi_d \rho f]^2}}{|D_2|}$$

$$|D_2| = \sqrt{([1-\rho^2][f^2-\rho^2] - \bar{m}\rho^2 f^2)^2 + (2\xi_d \rho f[1-\rho^2(1+\bar{m})])^2}$$

$$H_1' = \rho^2 H_1$$

$$H_1' = \frac{\sqrt{\rho^4[f^2-\rho^2]^2 + \rho^4(2\xi_d \rho f)^2}}{|D_2|} = \rho^2 H_1$$

$$q_1 = \rho^2[f^2-\rho^2] \qquad q_2 = \rho^2(2\rho f)$$

$$q_3 = ([1-\rho^2][f^2-\rho^2] - \bar{m}\rho^2 f^2)$$

$$q_4 = 2\rho f[1-\rho^2(1+\bar{m})]$$

$$H_1' = \sqrt{\frac{q_1^2 + \xi_d^2 q_2^2}{q_3^2 + \xi_d^2 q_4^2}} = \frac{q_2}{q_4}\sqrt{\frac{q_1^2/q_2^2 + \xi_d^2}{q_3^2/q_4^2 + \xi_d^2}} \Rightarrow H_1'|_{\rho\omega} = \left|\frac{q_2}{q_4}\right|$$

NOW TO MAKE H_1' INDEPENDENT OF ξ_d SINCE ALL POINTS WILL PASS THROUGH SAME POINT REGARDLESS OF DAMPING

$$\left|\frac{q_1}{q_2}\right| = \left|\frac{q_3}{q_4}\right|$$

$$\frac{\rho^2[f^2-\rho^2]}{\rho^2[2\rho f]} = -\frac{([1-\rho^2][f^2-\rho^2] - \bar{m}\rho^2 f^2)}{2\rho f[1-\rho^2(1+\bar{m})]}$$

$$[f^2-\rho^2]\cdot 2\rho f[1-\rho^2(1+\bar{m})] = -2\rho f\cdot([1-\rho^2][f^2-\rho^2] - \bar{m}\rho^2 f^2)$$

$$f^2 + f^2\rho^2 + f^2\rho^2\bar{m} + \rho^2 - \rho^4 - \rho^4\bar{m} - f^2 + \rho^2 + f^2\rho^2 - \rho^4 + \bar{m}\rho^2 f^2 = 0$$

$$+2f^2 - 2f^2\rho^2 - 2f^2\rho^2\bar{m} - 2\rho^2 + 2\rho^4 + \rho^4\bar{m} = 0$$

$$2\rho^4 + \rho^4\bar{m} - 2f\rho^2 - 2f^2\rho^2\bar{m} - 2\rho^2 + 2f^2 = 0$$

$$\rho^4(1+\tfrac{1}{2}\bar{m}) - f^2\rho^2 - f^2\rho^2\bar{m} - \rho^2 + f^2 = 0$$

$$\left(1+\tfrac{1}{2}\bar{m}\right)\rho^4 - \left(f^2 + f^2\bar{m} + 1\right)\rho^2 + f^2 = 0$$

$$\left(1+\tfrac{1}{2}\bar{m}\right)\rho^4 - \left[(1+\bar{m})f^2 + 1\right]\rho^2 + f^2 = 0$$

$$\rho^4 - \left[\left(\frac{1+\bar{m}}{1+0.5\bar{m}}\right)f^2 + \frac{1}{(1+0.5\bar{m})}\right]\rho^2 + f^2\frac{1}{(1+0.5\bar{m})} = 0$$

NOTICE: VERY SIMILAR TO QUADRATIC ON PAGE 237 FOR H_2. SMALL VALUES OF $\bar{m}$ WILL YIELD SAME RESULTS.

$$H_1'\big|_{PQ} = \left|\frac{a_2}{a_4}\right| = \left|\frac{\rho^2(2\rho f)}{2\rho f\left[1-\rho^2(1+\bar{m})\right]}\right| = \left|\frac{\rho^2}{\left[1-\rho^2(1+\bar{m})\right]}\right|$$

$$H_1'\big|_{PQ} = \frac{\rho_{1,2}^2}{\left|1-\rho_{1,2}^2(1+\bar{m})\right|} \quad \text{or} \quad H_1'\big|_{PQ} = \frac{1}{\left|\frac{1}{\rho_{12}^2} - (1+\bar{m})\right|}$$

WE KNOW THAT ρ_1 & ρ_2 @ SAME AMPLITUDE.

$$\frac{\rho_1^2}{1-\rho_1^2(1+\bar{m})} = \frac{\rho_2^2}{1-\rho_2^2(1+\bar{m})} \quad \text{or} \quad \left|\frac{1}{\rho_1^2} - (1+\bar{m})\right| = \left|\frac{1}{\rho_2^2} - (1+\bar{m})\right|$$

RECOGNIZING THAT $\rho_1 < 1$ & $\rho_2 > 1$

$$\frac{\rho_1^2}{1-\rho_1^2(1+\bar{m})} = \frac{\rho_2^2}{\rho_2^2(1+\bar{m})-1} \quad \text{or} \quad \frac{1}{\rho_1^2} - (1+\bar{m}) = (1+\bar{m}) - \frac{1}{\rho_2^2}$$

$$\frac{\rho_1^2+\rho_2^2}{\rho_1^2\rho_2^2} = 2(1+\bar{m})$$

NOW SOLVE QUADRATIC ABOVE

$$r_{1,2} = \frac{-b \pm \sqrt{b^2-4ac}}{2a}$$

$$r_1+r_2 = \left(\frac{-b}{2a} + \frac{\sqrt{b^2-4ac}}{2a}\right) + \left(\frac{-b}{2a} - \frac{\sqrt{b^2-4ac}}{2a}\right) = -\frac{2b}{2a} = -b$$

$$r_1 r_2 \quad \frac{b^2 + bd - bd - d^2}{4}$$

$$\frac{r_1+r_2}{r_1 r_2} = \frac{+b}{b^2-d^2} = \frac{4b}{b^2-(b-4)}$$

$$\frac{4\left[\left(\frac{1+\bar{m}}{1+0.5\bar{m}}\right)f^2+\left(\frac{1}{1+0.5\bar{m}}\right)\right]}{\left[\left(\frac{1+\bar{m}}{1+0.5\bar{m}}\right)f^2+\left(\frac{1}{1+0.5\bar{m}}\right)\right]^2-\left[\left(\frac{1+\bar{m}}{1+0.5\bar{m}}\right)f^2+\left(\frac{1}{1+0.5\bar{m}}\right)-4\left(\frac{1}{1+0.5\bar{m}}\right)\right]}=\frac{f_1^2+f_2^2}{f_1^2 f_2^2}$$

$$\alpha=\frac{1+\bar{m}}{1+0.5\bar{m}} \qquad \beta=\frac{1}{1+0.5\bar{m}}$$

$$\frac{4\left[\alpha\beta f^2+\beta\right]}{\left[\alpha\beta f^2+\beta\right]^2-\left[\alpha\beta f^2+\beta-4\beta\right]}=\frac{4\left[\alpha\beta f^2+\beta\right]}{\left[\alpha\beta f^2+\beta\right]^2-\left[\alpha\beta f^2-3\beta\right]}$$

$$=\frac{4\beta\left(\alpha f^2+1\right)}{\beta\left[\beta\left(\alpha f^2+1\right)^2-\left[\alpha f^2-3\right]\right]}=2\alpha$$

$$=\frac{2\left(\alpha f^2+1\right)}{\beta\left(\alpha f^2+1\right)^2-\left(\alpha f^2-3\right)}=\alpha$$

$$2\alpha f^2+2=\alpha\beta\left(\alpha^2 f^4+2\alpha f^2+1\right)-\alpha f^2+3$$

$$\alpha^2\beta f^4+2\alpha^2\beta f^2+\alpha\beta-\alpha f^2+3-2\alpha f^2+2=0$$

$$\alpha^2\beta f^4+\left(2\alpha^2\beta-\alpha-2\alpha\right)f^2+\alpha\beta+5=0$$

$$f^4+\left(\frac{2}{\alpha}-\frac{3}{\alpha^2\beta}\right)f^2+\left(\frac{1}{\alpha^2}+\frac{5}{\alpha^3\beta}\right)=0$$

10. Appendix D: Tuned Mass Damper Design Calculations

Tuned Mass Damper Design

Design a Tuned Mass Damper given an acceleration Constraint of 0.005g, 0.01g, and 0.015g and compare results.

$g := 9.81 \qquad p := 290 \quad N$

$$a := \begin{pmatrix} 0.005\,g \\ 0.01 \cdot g \\ 0.015\,g \end{pmatrix}$$

$$H'_1 := \frac{a}{PM_{actual}}$$

$$H'_1 = \begin{pmatrix} 2.461 \\ 4.922 \\ 7.383 \end{pmatrix}$$

Now go to H'1 chart below and obtain mass ratio. From here proceed to following charts to obtain optimal values.

	0.5% g	1% g	1.5% g
H_{1opt}	2.5000	4.9000	7.4000
$\bar{m}$	N/A	0.0750	0.0340
f_{opt}	N/A	0.9640	0.9830
ξ_{dopt}	N/A	0.146	0.110
ξ_e	N/A	0.100	0.067

	0.5% g	1% g	1.5% g
m_d (kg)	N/A	48.75	22.10
ω_d (rad/s)	N/A	32.10	32.73
k_d (kN/m)	N/A	50.24	23.68
c_d (N-s/m)	N/A	456.97	159.16